NOVA SCHOOL OF SCIENCE & TECHNOLOGY

DEPARTMENT OF MATERIALS SCIENCE

MARTA VILAR SARAIVA MATEUS

Bachelor of Science in Micro and Nanotechnology Engineering

SUPERPARAMAGNETIC IRON OXIDE "NANOZYMES" FOR CANCER THERANOSTICS

MASTERS IN MICRO AND NANOTECHNOLOGIES ENGINEERING

Universidade NOVA de Lisboa

April, 2022

SUPERPARAMAGNETIC IRON OXIDE “NANOZYMES” FOR CANCER THERANOSTICS

MARTA VILAR SARAIVA MATEUS
Bachelor of Science in Micro and Nanotechnology Engineering

Advisor: Dra. Paula Isabel Pereira Soares,
Researcher, NOVA University Lisbon

Co-advisor: Professor Dr. Jorge Carvalho e Silva,
Associate Professor, NOVA University Lisbon

Examination Committee

Chair: Professor Dr. Rodrigo Ferrão de Paiva Martins

Rapporteur: Professor Dr. João Paulo Miranda Ribeiro Borges

Member: Dra. Paula Isabel Pereira Soares

MASTERS IN MICRO AND NANOTECHNOLOGIES ENGINEERING

Universidade NOVA de Lisboa
June, 2022

Superparamagnetic Iron oxide "nanozymes" for cancer theranostics

ACKNOWLEDGMENTS

Em primeiro lugar gostaria de agradecer à minha orientadora, Professora Paula Soares e coorientador Professor Jorge Silva, não só por toda a disponibilidade e apoio prestado ao longo destes meses, mas também por todos os conselhos e apoio que me deram durante os tempos mais difíceis quando tudo parecia correr mal e por me terem guiado para melhores soluções.

Ao Professor João Paulo Borges por me ter acolhido no seu laboratório e me ter dado a oportunidade de desenvolver este tema e à Professora Susana Barreiros por me ter facultado o acesso, indispensável, ao laboratório 427 (DQ).

Obrigada a todos os meus colegas do laboratório de polímeros (DCM), em especial à Adriana e à Catarina por toda a ajuda e disponibilidade sempre. Um enorme obrigada a todas do laboratório de células e tecidos (DF), Tânia, Thais, Lya e Sofia por me terem ajudado e ensinado tanto, mas também pelos momentos bons de convívio e boa disposição que animavam sempre o meu dia.

Um grande beijinho às minhas amigas de faculdade pelas horas passadas a estudar na faculdade e no skype e por todos os momentos épicos que tivemos, sem vocês teria sido muito mais complicado sobreviver a estes 5 anos. Tenho a certeza de que vos levo para o resto da vida! Bia, o maior obrigada de sempre por todo o apoio que me deste agora nos últimos meses, foste sempre incansável e não teria chegado ao fim sem ti!!

Às loucas da minha vida, Zinha e Bi, que estão sempre ao meu lado prontas para me ouvirem, apoiarem e me darem na cabeça, vocês são as melhores!!

Por fim, o maior obrigada à minha família, mãe, pai e Sofi por todo o apoio incondicional e motivação que me deram, estiveram lá sempre para me ajudar nos momentos mais baixos mas também para celebrar as minhas conquistas, adoro-vooos!! Agradeço também ao

João, por acreditares sempre em mim e não me deixares desmotivar.

"Ever tried. Ever failed. No matter. Try again. Fail again. Fail better."
(Samuel Beckett)

ABSTRACT

Cancer is the second most prevalent cause of death worldwide. Chemotherapy and radiotherapy are some of the most commonly used treatments. They, however, present serious side effects for the patient. As technology evolves, new possibilities for cancer treatment arise. In this sense, cancer theranostics provides the possibility of having diagnosis and treatment in a single system, improving patient care, and providing personalized cancer treatment methods. One of the most promising approaches to theranostics is using superparamagnetic iron oxide nanoparticles (SPIONs) as they can be used as contrast agents in magnetic resonance imaging and in magnetic hyperthermia due to the increase of their bulk temperature and of their surroundings when an external alternating magnetic field is applied. More recently, it was discovered that SPIONs mimic peroxidase and catalase enzymatic activities. The first one contributes to direct tumour elimination by generating toxic radicals while the latter converts hydrogen peroxide into water and oxygen, helping overcome the hypoxia present in tumour tissues.

In this work, SPIONs were coated with dimercaptosuccinic acid and 3-amino-propyltriethoxysilane and characterized. The peroxidase and catalase enzyme-like activity of coated SPIONs was also evaluated as well as the influence that various pH and different hydrogen peroxide concentrations have on the enzymatic-like activity. After this characterization, cytotoxic assays were performed using the SaOs-2 cell line with SPIONs and hydrogen peroxide to determine which are the cytotoxic concentrations for both. The main goal was to assess the *in-vitro* catalase-like behaviour of SPIONs in normoxia and hypoxia environments. Lastly, the SPIONs were submitted to an alternating magnetic field and hyperthermic temperatures were reached.

Here, we showed that SPIONs possess intrinsic catalase and peroxidase like activities, however the same was not achieved in *in-vitro* studies. In this sense, more studies are required to accurately assess catalase-like activity *in vitro*, as well as more in-depth magnetic hyperthermia assays including *in-vitro* to better understand SPIONs as theranostics system.

Keywords: Cancer, Catalase, *IONzymes*, Magnetic hyperthermia, Peroxidase, Superparamagnetic nanoparticles, Theranostics.

RESUMO

O cancro é a segunda maior causa de morte em todo o mundo. A quimioterapia e a radioterapia são alguns dos tratamentos mais utilizados. Porém, apresentam graves efeitos secundários para o paciente. À medida que a tecnologia evolui, surgem novas possibilidades para o tratamento do cancro. Nesse sentido, o teranóstico oferece a possibilidade de diagnóstico e tratamento num único sistema, melhorando o atendimento ao paciente e oferecendo métodos personalizados de tratamento do cancro. Uma das abordagens mais promissoras para o teranóstico é o uso de nanopartículas superparamagnéticas de óxido de ferro (SPIONs), por poderem ser usadas como agentes de contraste em ressonância magnética e em hipertermia magnética devido ao aumento de sua temperatura e do ambiente em redor aquando da aplicação de um campo magnético externo alternado. Mais recentemente, descobriu-se que as SPIONs conseguem mimetizar as atividades enzimáticas da peroxidase e da catalase. O primeiro contribui para a eliminação direta do tumor através da geração de radicais tóxicos enquanto o segundo converte o peróxido de hidrogénio em água e oxigénio, ajudando a diminuir a hipóxia presente nos tecidos tumorais.

As SPIONs foram revestidas com ácido dimercaptossuccínico e 3-amino-propiltrietoxissilano e posteriormente caracterizadas. A atividade enzimática de peroxidase e catalase das SPIONs revestidas também foi avaliada, bem como a influência que vários pH e diferentes quantidades de peróxido de hidrogénio têm na atividade enzimática. Após esta caracterização, foram realizados ensaios citotóxicos na linhagem de células SaOs-2 com SPIONs e peróxido de hidrogénio, aqui foi determinado quais eram as concentrações citotóxicas para ambos. O objetivo principal foi avaliar o comportamento de catalase dos SPIONs *in vitro* em ambientes de normóxia e hipóxia. Por fim, os SPIONs foram submetidos a um campo magnético alternado e foram atingidas temperaturas hipertérmicas.

Aqui, mostramos que as SPIONs possuem atividades intrínsecas de catalase e peroxidase, porém o mesmo não foi alcançado em estudos *in vitro*. Nesse sentido, são necessários mais estudos para avaliar com precisão a atividade de catalase *in vitro*, bem como ensaios de hipertermia magnética mais aprofundados, incluindo *in vitro*, para entender melhor SPIONs como sistema de teranóstico.

Palavras-chave: Cancro, Catalase, *IONzymes*, Hipertermia magnética, Peroxidase, Nanopartículas superparamagnéticas, Teranóstico.

CONTENTS

LIST OF FIGURES

LIST OF TABLES

ABREVIATIONS

AMF	Alternating magnetic field
APTES	3-Amino-propyl-triethoxysilane
CAT	Catalase
DLS	Dynamic light scattering
DMSA	Dimercaptosuccinic Acid
DMSO	Dimethyl Sulfoxide
DNA	Deoxyribonucleic Acid
FBS	Fetal bovine serum
FTIR	Fourier Transform Infrared spectroscopy
HIF(s)	Hypoxia-inducible-factor(s)
HEPES	4-(2-hydroxyethyl)-1-piperazineethanesulfonic acid
HRP	Horseradish peroxidase
ION	Iron Oxide Nanoparticle
IONzyme(s)	Iron Oxide Nanozyme(s)
MRI	Magnetic resonance imaging
NP(s)	Nanoparticle(s)
PBS	Phosphate Buffer Saline
PDI	Polydispersity index
ROS	Reactive Oxygen Species
SPIONs	Superparamagnetic Iron Oxide Nanoparticles
SPIONs_APTES	Superparamagnetic Iron Oxide Nanoparticles stabilized with (3-Aminopropyl) triethoxysilane
SPIONs_DMSA	Superparamagnetic Iron Oxide Nanoparticles stabilized with Di-mercaptosuccinic acid
TEM	Transmission Electron Microscopy
TMB	3,3′,5,5′-Tetramethylbenzidine
TME	Tumor Microenvironment
UV-Vis	Ultraviolet spectrophotometry
XRD	X-Ray Diffraction

1. MOTIVATION

Cancer is a worldwide disease and the number one cause of death, causing 10 million fatalities across the world [1]. Facing these numbers, finding a cancer treatment option is of the at most importance and significant advances have been done over the years.

In this context, cancer theranostics has gained more importance as it combines diagnostic and treatment features in one single technology, aiming to decrease treatment delays and improve patient care [2]. Moreover, the use of nanotechnology for biomedical applications has been a topic of research for the past years, namely magnetic nanoparticles (NPs) demonstrate a huge potential to significantly improve theranostics platforms for cancer. Their unique properties, enable their use as imaging probes in the diagnostic feature, and as magnetic hyperthermia agents in the treatment feature [3].

Recently, superparamagnetic iron oxide nanoparticles (SPIONs) have been studied for their intrinsic enzyme-like properties either peroxidase-like or catalase-like, being referred as IONzymes, IONzymes can contribute to direct tumour elimination through its intrinsic peroxidase-like activity, which leads to the generation of toxic radicals. On the other hand, catalase like activity results in the decomposition of H_2O_2 into oxygen and water, resulting in an increase in the oxygen concentration in tumour environment, can help reverse hypoxia induced resistance of tumours to treatment, namely chemotherapy [4], [5].

The work in here presented was divided into four stages:

1. Synthesis of superparamagnetic iron oxide nanoparticles (SPIONs), by chemical co-precipitation and further characterization;
2. Cytotoxicity Studies of SPIONs and H_2O_2;
3. Qualitative and quantitative study of SPIONs cellular internalization;
4. Enzymatic-like assays chemical and intracellularly;
5. Magnetic hyperthermia studies to assess feasibility of SPIONs for cancer treatments.

2. INTRODUCTION

2.1. Cancer

According to the World Health Organization, cancer is the second leading cause of death around the world. The most common cancers are breast, lung, colon, and prostate cancers, responsible for more than 7 million new cases in 2020. In Portugal alone there were 60467 new diagnoses and 30168 deaths in 2020 [1].

Most healthy cells follow a cycle which begins when a single cell divides into two daughter cells. The progression of the cell cycle is regulated by signals from outside and within cells. Interrupting or altering these signals can lead to changes within the cells, including transformation into malignant cells [6]. Tumors are not just formed by malignant cells masses, they are also composed by cells of the immune system, the tumor vasculature, and lymphatics, as well as fibroblasts, pericytes which form the tumor microenvironment (TME) [7]. A common characteristic of solid TME is the uncontrolled cell proliferation that exceeds the ability to satisfy the oxygen demand, leaving the TME with a low oxygen supply also known as hypoxia [8]. Hypoxic tumors often present high levels of reactive oxygen species (ROS), such as hydrogen peroxide (H_2O_2), superoxide anion (O_2^-), and the hydroxyl radical (OH^-); low pH and altered metabolism [9].

Cancer treatments have been developed over the decades, the most common treatment options are chemotherapy and radiotherapy however, their side effects can be very harsh and cause more suffering to the patient, hence the necessity of discovering new and improved treatments. In recent years, nanotechnology emerged in the biomedicine field, more in particular superparamagnetic nanoparticles as they hold interesting features that can be used for medical purposes [10].

2.2. Superparamagnetic iron oxide nanoparticles

Magnetic nanoparticles are a class of nanoparticles that possess magnetic sensitivity and therefore can be oriented and controlled under an externally applied magnetic field. In this class of nanoparticles, SPIONs are the ones that have shown more potential in biomedical applications [3] such as magnetic resonance imaging (MRI), magnetic hyperthermia, drug carrier in target tumor treatments [3]. SPIONs consist of a magnetic core, usually magnetite (Fe_3O_4) or maghemite (γ-Fe_2O_3) and a biocompatible coating [11]. These nanoparticles tend to change their oxidation state, agglomerate, and lose their magnetic properties over time and so, coating them is essential to give chemical stability and long-term stability [12]. For magnetite, magnetization occurs due to the presence of iron cations in two states of valence, Fe^{2+} and Fe^{3+} and their electronic movement [13]. The superparamagnetic property of these nanoparticles arises when their size is < 15 nm

(critical size) and they hold a core that consists in a single magnetic domain, in which all the atomic magnetic moments are magnetized in the same direction and behave as a single magnetic dipole, thus having a large magnetic moment. Therefore, when exposed to an external magnetic field they become intensely magnetized and rapidly lose their magnetization when the field is no longer present [14]. In addition, SPIONs are biocompatible, biodegradable and have low cytotoxicity, which are crucial characteristics for *in vivo* applications. These nanoparticles assume a high surface area-to-volume ratio and high aspect ratio values, a relevant feature for cellular internalization and surface functionalization [3].

In addition to high magnetization (between 30 and 50 emu/g) [15], SPIONs also have the ability to heat when an alternating magnetic field (AMF) is applied. Heating occurs during the demagnetization process due to energy loss [14]. This property is explored in hyperthermia treatments for cancer. Hyperthermic treatments aim to kill tumor cells whilst keeping healthy cells unharmed. The hyperthermia treatment intends to increase the temperature of a certain area or whole body to 42º-45º by the application of electromagnetic field techniques, ultrasound, or microwaves. This is possible because cancer cells have a high glycolytic activity and consequently lower pH than normal cells, which confers the cancer cells a superior sensitivity to heat [16]. Hyperthermia using SPIONs is possible, as mentioned above, when an external alternating magnetic field is utilized. This field will trigger mechanisms such as: hysteresis losses, Neél relaxation, Brownian relaxation, and frictional losses which will increase the temperature, allowing it to kill the cancer cells [17].

Besides the strong bet on SPIONs for cancer theranostics, researchers have also been investigating the option of using biological enzymes for cancer treatments or as cancer treatment boosters [18], [19].

2.3. Catalase and Peroxidase

In aerobic forms of life, the production of energy generates H_2O_2 and other ROS which can be toxic to the system. H_2O_2, in particular, has been found to be part of the cell's signaling cascade when in low concentrations, but can be very toxic when in high concentrations [20]. As a form of stabilizing and dissociating these ROS, eucaryotic cells developed antioxidant enzymes. Catalase (CAT) is an enzyme that can be found in the peroxisomes of animal cells and decomposes H_2O_2 in water and oxygen (equation 2.1). Peroxidase is another enzyme that, like catalase, plays a critical role in preventing cellular oxidative damage in aerobically respiring organisms, therefore reducing the toxicity in the area. This enzyme uses H_2O_2 as a substrate and creates free radicals to react with hydrogen donors (equation 2.2) [21]. In equation 2.2 peroxidase, A represents a generic chemical element.

Catalase $$2H_2O_2 \rightarrow 2H_2O + O_2 \quad (2.1)$$

Peroxidase $$H_2O_2 + 2AH \rightarrow 2H_2O + 2A \quad (2.2)$$

Reactive oxygen species are very important for cell function: low concentration of ROS promotes cell proliferation and survival, while intermediate concentration induces cell differentiation. But at high concentrations, ROS can produce oxidative damage, especially in the DNA, causing mutations which eventually lead to cancer. Cancer sites are characterized by persistent metabolic reactions leading to high ROS concentrations that antioxidant enzymes are unable to regulate due to their under expression, thus promoting cancer cells proliferation. In a general sense, ROS can be responsible for cancer development and play a crucial role in its proliferation. This demonstrates the importance of developing new treatment options to reduce ROS concentrations [22].

Christophe Glorieux *et. al*. studied the effects of overexpressed catalase in breast tumor cells. They found that the overexpression of catalase does increase catalase activity and that the overexpressed catalase reduced cell proliferation and mitigation, indicating that ROS levels had been diminished as they are crucial for tumor growth. In addition, the influence of over expressed catalase in regular cancer treatment options such as chemo and radiotherapy were also evaluated. It was concluded that these cells demonstrate higher sensitivity towards some chemotherapeutic agents however did not show any changes when exposed to ionizing radiation [18].

In another study, Chao Shi *et al.* utilized a liposomal encapsulated catalase together with lyso-targeted NIR photosensitizer (MBDP) and doxorubicin (Dox) to increase tumor O_2 levels, their studies were done on mice implanted with tumor cells. They showed, by fluorescent markers, that the marked hypoxia regions decreased three days after being injected with the liposomal encapsulated catalase thus proving that H_2O_2 was being catalyzed to produce O_2 and consequently alleviating tumor hypoxia. After hypoxia reduction, they combined chemo and photodynamic therapy which enhanced the tumor therapeutic effect by promoting chemo-PDT and antitumor immunities [23].

Regarding peroxidase enzymes in cancer therapies, Jingru Liu *et al*. investigated how glutathione peroxidase could reduce growth of pancreatic cancer cells. They performed *in vitro* and *in vivo* studies in mice and reached the conclusion that in both cases, the use of overexpressed glutathione peroxidase did indeed reduce cell growth in over 50%, due to the reduction of the malignant phenotype, consequence of deregulated gene expression common in cancer cells [19].

These are some examples that show and prove that the use of enzymes can be a cancer therapeutic option. As mentioned before, enzyme have great purpose however, their high cost of synthesis, isolation, and purification as well as their lack of stability in various environments (temperature and pH variations) lead the scientific community to study other options [24]. One of those options were inorganic nanoparticles that could mimic the enzymatic activity, namely, SPIONs have been studied for their intrinsic peroxidase-like and catalase-like activities under physiological conditions, denominated "IONzymes" [25] .

2.4. "IONymes"

When comparing IONzymes with natural enzymes, IONzymes present some advantages such as more stability, low cost, and mass-production, allowing for more possibilities in future applications [25].

2.4.1. Peroxidase-like activity

Gao *et al.* were the first group of researchers that studied Fe_3O_4 NPs and their intrinsic peroxidase activity. In this article Gao *et al.* compared the activity of horseradish peroxidase (HRP) and Fe_3O_4 NPs through enzymatic assays (oxidation of substrates; pH, temperature, size and H_2O_2 concentration dependence; reaction mechanisms) and in the end was able to say that Fe_3O_4 NPs beyond doubt have intrinsic peroxidase-like activity and are identical to the HRP enzyme [4].

Years later, *Wang et al.* started by identifying the ROS and worked backwards to understand the reactions that originated those ROS. As a result, $^{\bullet}OH$, and $O_2^{-\bullet}/HO_2^{\bullet}$ radicals were the main ROS that resulted from the reaction and $O_2^{-\bullet}/HO_2^{\bullet}$ are the major reactive radicals. The general catalytic mechanism for the activation of H_2O_2 by Fe_3O_4 is the following [26] :

$$Fe^{III}(P)^{+} + H_2O_2 \rightarrow Fe^{III}(P)(H_2O_2)^{+} \rightarrow Fe^{IV}(P)(P^{\cdot -})(O)^{+} + H_2O \quad (2.3)$$

$$Fe^{IV}(P^{\cdot -})(O)^{+} + AH_2 \rightarrow Fe^{IV}(P)(O) + HA^{\cdot} + H^{+} \quad (2.4)$$

$$Fe^{IV}(P)(O) + AH_2 \rightarrow Fe^{III}(P^{+})(O) + HA^{\cdot} + OH^{-} \quad \text{or} \quad (2.5)$$

$$2H^{\cdot} \rightarrow A + AH_2 \quad \text{or} \quad (2.6)$$

$$2H^{\cdot} \rightarrow HA - AH \quad (2.7)$$

Peroxidase reaction under physiological conditions is considered to be oxidized in a single-electron step (Equations 2.4 and 2.5), the final result is through disproportionation (Equation 2.6) or coupling (Equation 2.7) of the single electron oxidation intermediate [27].

Overall, the discovery of peroxidase-like activity in SPIONs showed that these NPs are bioactive and have advantages when compared to natural enzymes. Some of the advantages are the fact that SPIONs are inorganic, tolerating a harsher environment: they tolerate a wider range of pH (3 - 5.5) and temperatures (35 - 50 ^{o}C) and still have a good enzymatic activity; "nanozymes" are more cost effective as they are easier to produce and allow for surface modification [4], [28]. Synthesis of SPIONs is a very important step as the type of reaction and its conditions determine the size and shape of the NPs. Size is a critical characteristic of the nanozyme because it determines the amount of activity that they possess (smaller particles exhibit more activity) [29], [30].

2.4.2. Catalase-like activity

Chen et al. investigated peroxidase-like activity of Fe_3O_4 NP at different pH: 4.8 and 7.4 using a 3,3',5,5'-tetramethylbenzidine (TMB) assay, where the TMB, in the presence of H_2O_2, is catalyzed by the nanoparticle and the color changes to blue. At pH 4.8, the color change was verified, but at 7.4 the solution remained transparent. Instead, after 30 min of incubation, some gas bubbles started to appear and after a few hours they had

grown bigger. The presence of the gas bubbles and the fact that the solution did not change its color came to prove that at a neutral pH the nanoparticles do not possess peroxidase activity but do have a catalase-like activity. Thus, reaching the conclusion that Fe_3O_4 NP have a dual enzymatic activity, peroxidase-like activity at acidic pH (3-5.5) and a catalase-like activity at a neutral pH (7.4) [31].

The shift in the activity most likely has to do with the pH. When the environmental pH changes to neutral or basic, the Fe^{3+} content in the iron-based nanozymes becomes the dominant catalytic species, favoring the catalase-like decomposition of H_2O_2.Thus the reaction of catalase-like activity is [32]:

$$Fe^{III}(P)^{+}+H_2O_2 \rightarrow Fe^{III}(P)(H_2O_2)^{+} \rightarrow Fe^{IV}(P)(P^{\cdot -})(O)^{+}+H_2O \quad (2.3)$$

$$Fe^{IV}(P^{\cdot -})(O)^{+}+H_2O_2 \rightarrow Fe^{III}(P)^{+}+H_2O+O_2 \quad (2.9)$$

In the catalase reaction, it has been determined that the molecular oxygen formed is caused by hydrogen peroxide, which means that no O-O bond rupture occurs in Equation 2.9. Therefore, this is the two-electron reduction of compound I ($Fe^{IV}(P^{\cdot -})(O)+$), namely produced by the reaction of ferric iron in enzymes with hydrogen peroxide. With hydrogen peroxide, the oxo ligand of the former is released in the form of water [27].

2.4.3. *In vitro* enzymatic-like activity

After assessing the enzymatic-like activity of SPIONs, it is important to understand if they have the same results *in vitro* to understand their applicability in biomedicine. As previously stated, treatments efficacy is impeded by the tumor's intrinsic resistance to chemotherapeutic agents. A major physiological contributor to drug resistance is the low oxygen availability in tumor sites. Hypoxia-inducible factors (HIFs) are key regulators of oxygen levels within tissue, and its expression is induced under hypoxic conditions which makes HIFs ideal targets for reducing drug resistance. In 2019, Tin-Yo Yen *et al*. studied if catalase-functionalized iron oxide nanoparticles (CAT-ION) could reverse hypoxia-induced chemotherapeutic resistance. This group utilized catalase-functionalized iron oxide nanoparticles as they found that the combination of both boosted the desired catalase activity. Tin-Yo Yen *et al.* found that CAT-ION reduced the expression of HIFs in breast cancer cells *in vitro*, confirming functional catalase activity. Furthermore, breast cancer cells demonstrated considerable decrease in drug resistance [5].

In a different approach, Shanshan Gao *et al.* used Au NPs and Fe_3O_4 NPs integrated into dendritic mesoporous silica NPs (DMSN-Au-Fe_3O_4 NPs) for tumor therapy. Even though the concentration of H_2O_2 is much higher than the desirable it is not sufficient to produce enough hydroxyl radicals for inducing satisfactory nanocatalytic-therapeutic. So, this research group combine the glucose oxidase-like activity of Au to elevate the intratumoral H_2O_2 concentration and peroxidase-like activity of Fe_3O_4 that turns the H_2O_2 into hydroxyl radicals and thus inducing cancer cells death, forming a dual inorganic nanozyme-triggered TME-responsive cascade catalytic reaction for efficient nanocatalytic tumor therapy [33].

Given all the developments achieved to this day in the nanozyme field, this project aims to take advantage of both enzymatic like activities (catalase and peroxidase) of SPIONs to simultaneously reduce hypoxia in TME to increase chemotherapy treatments efficacy and produce hydroxyl radicals, inducing cancer cells death.

3. MATERIALS AND METHODS

3.1. Superparamagnetic iron oxide nanoparticles

3.1.1. Synthesis

SPIONs were synthesized via chemical co-precipitation. The reagents $FeCl_3.6H_2O$: 10 mmol and $FeCl_2.4H_2O$: 5 mmol (Alfa Aesar) were dissolved in Millipore water, 20 mL and 5 mL respectively, and in the end another 50 mL of water was added to the solution in other to obtain a 1:2 Fe^{2+}: Fe^{3+} molar ratio. Inside a hood, the mixture was put under a mechanical stirring, with O_2 deaeration and with bubbling N_2. It is important to have an environment free of oxygen during the synthesis otherwise maghemite is formed. 10 mL of ammonia 25% (Sigma-Aldrich) were added to the mixture for NPs growth and the mixture was left under mechanical stirring (600 rpm) for 5 min. After that time, 60 mL of water were added to stop the reaction. The NPs were separated from the supernatant and washed 5 times with distilled water, with the aid of a magnet [34]. SPIONs obtained by this method have low stability in aqueous solution. So, SPIONs were coated with two different stabilizers: 10% (v/v) of (3-aminopropyl) triethoxysilane (APTES) and 13 mM of dimercaptosuccinic acid (DMSA). The stabilization protocols of the SPIONs and their as well as their quantifications protocol are specified in Appendix A and B respectively.

3.1.2. Characterization

FTIR spectra of the nanoparticles was obtained using a Nicolet 6700 FT-IR spectrometer from Thermo Scientific with a range of 4000 cm^{-1}- 500 cm^{-1}.

The XRD patterns were recorded using the Rigaku MiniFlex+ Desktop X-ray diffractometer (MiniFlex+, Rigaku, Tokyo, Japan) using Cu-Kα radiation generated at 45 kV and 40 mA, in the range of $10º<2\theta<90º$ with a step of 0.033º.

Zeta potential and DLS measures were performed using a SZ-100 nanopartica series (Horiba, Lda) with a laser of 532 nm and controlling temperatures with a Peltier system (25 ºC).

Using magnetic hyperthermia device (NanoScale Biomagnetics, DM100 Series) the generated temperature of the SPIONs was measured by applying an alternating magnetic field of 300 Gauss with a frequency of 418.5 kHz. The measurements lasted 10 minutes. The studies were done for SPIONS in Millipore water and in McCoy culture cell medium with concentrations of 0.05 mg/mL; 0.1 mg/mL; 0.5 mg/mL; 1 mg/mL.

3.2. Chemical Catalase and Peroxidase assay

The peroxidase-like activity assays were carried out in 3 mL plastic cuvettes, where to 2 mL phosphate buffer (100 mM, pH 5.5) were added a specific volume of a 5 mg/mL monodisperse solution of NPs, using a given amount of 10 mg/mL solution of TMB (Sigma-Aldrich) as the substrate, and in the presence of 25 µL H_2O_2 (Sigma-Aldrich) 8.8 M. The absorbance was measured at 652 nm using a UV-VIS spectrophotometer (GENESYS 50 UV-Vis Spectrophotometer Thermo Fisher Scientific) [4].

The catalase-like activity was measured using, to 1 mL of Phosphate Buffer Saline (PBS) (pH 7.4), 40 µL of a monodisperse solution of NPs were added. Then 2 µL of hydrogen peroxide was added to the reaction, and the absorbance was measured at 240 nm for thirty minutes, in ten-minute intervals [31].

3.3. Cell Culture

The cell line used in all studies was SaOs-2 (primary osteogenic sarcoma). Cells were grown in McCoy 5A medium (Sigma-Aldrich), supplemented with 10% fetal bovine serum (FBS) (Sigma-Aldrich) and 1% penicillin (100 U/mL) and streptomycin (100 µg/mL) (Invitrogen). Depending on the final study different densities were seeded on the plates. Once the seeding was complete the plate was put 24 h inside an 5% CO_2 incubator (Sanyo MCO19AIC(UV)) at 37 ºC. The different densities of cells that were seeded are described in Appendix C. The next day, the medium was removed from the wells and replaced with fresh culture medium containing a known concentration of the substrate in analysis, if using SPIONs, the medium used contained a fungicide (FUNGIZONE®), Amphotericin B (Gibco) solution (to prevent fungal contamination), gentamicin (Gibco) (to prevent the contamination of cell culture by bacteria). The plates were again left in the incubator.

3.4. Cytotoxicity

To assess cell viability in the presence of SPIONs_DMSA and SPIONs_APTES two cell viability tests were done: resazurin and Live/Dead assay. The followed protocols are described in Appendix D.

3.5. Cellular uptake: Prussian Blue and Intra cellular quantification

SPIONs dynamic of internalization was assessed by Prussian Blue staining and intra cellular quantification. The procedures followed are briefly described in Appendix E.

3.6. Catalase *in vitro* assay

After cell culture, SPIONs APTES and DMSA were added to the cells at a concentration of 0.03 mg/mL and were internalized. To measure catalase-like activity *in vitro*, 50 μM of H_2O_2 was added to the wells and incubated for three different time periods (30 min; 1 h; 1 h 30 min) following resazurin procedure to measure cell viability.

4. RESULTS AND DISCUSSION

4.1. SPIONs characterization

After the synthesis of SPIONs, morphological, chemical composition and size distribution characterization assays were carried out. FTIR analysis allows to identify the chemical groups present in the sample through vibration modes characteristic of the chemical bond as, for each material there is a different atom combination. In Figure 4.1 a typical absorbance band can be identified at 560 cm^{-1} corresponding to the stretching vibration mode of the Fe–O bond, related to the NPs´ iron oxide core. Another common vibration mode belongs to the broad band between 3000 cm^{-1} and 3500 cm^{-1} related to the O-H stretching vibration mode due to water vapor. Naked SPIONs present another O-H bond at 1590 cm^{-1} referent to this bond´s stretching vibration modes [34]. As for the coated SPIONs, the identified chemical bonds belong to the predominant functional group of each stabilizer. DMSA was identified by the characteristic asymmetric and symmetric stretching vibration modes of C=O groups at 1570 cm^{-1} and 1360 cm^{-1}, respectively thus confirming its presence on the SPIONs surface [35]. Regarding APTES coated SPIONs, the band at 1630 cm^{-1} corresponds to the N-H bending mode, while the absorbance band around 1100 cm^{-1} is due to the stretching vibration of Si–O, confirming the successful coating of the naked NP [36].

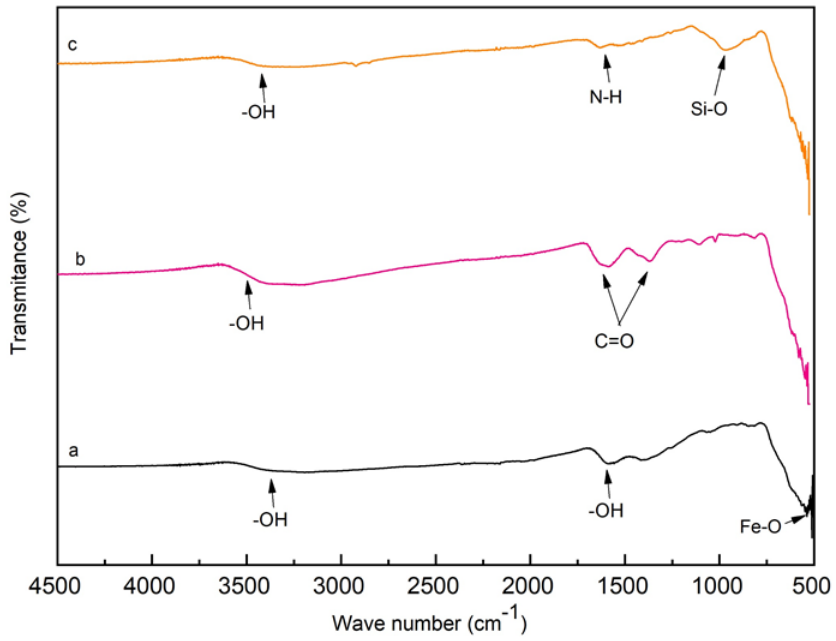

Figure 4.1: **FTIR spectra of iron oxide nanoparticles**. Naked NPs (a), DMSA coated NPs (b), APTES coated NPs (c).

Through the diffractograms in Figure 4.2 obtained by XRD analysis, one can study the crystalline structure of the NPs by identifying characteristic peaks. The peaks identified are associated with crystallographic planes according to the crystallographic

sheets of maghemite and magnetite powders (JCPDS 00-019-0629 for magnetite and JCPDS 00-039-1346 for maghemite). For the naked SPIONs, six characteristic peaks were found at 2θ equal to 30.3, 35.6, 43.3, 53.6, 57.2 and 63.1, equivalent to (220), (311), (400), (422), (511) and (440) diffraction planes, respectively [34]. Through Figure 4.2, it is also possible to say that after surface modification with the two different coatings, the characteristic peaks did not change, therefore the crystalline structure was not compromised. Magnetite and maghemite have very similar identical crystalline structures and can be hard to distinguish them. Despite that, comparing both crystallographic sheets it is possible to say that the synthesized SPIONs have a crystalline cubic structure mainly formed by magnetite. This can be justified due to the anaerobic environment of the NPs synthesis, which prevents magnetite oxidation to maghemite.

The average crystallite size, τ, was calculated for all three types of NPs using Scherrer's equation:

$$\tau = K\lambda\beta\cos(\theta) \tag{4.1}$$

Where K is the grain shape factor (K = 0.94); λ is the incident X-ray wavelength (λ = 1.54 Å); β denotes the full width at half-maximum (in radians) of the highest intensity, and θ is the corresponding diffraction angle [37]. The average crystallite size obtained for naked Fe_3O_4 SPIONs was 8.7 nm (2θ = 35.56), 8.7 nm (2θ =35.69) for APTES stabilized SPIONs and 9.7 nm (2θ = 35.79) for DMSA coated SPIONs.

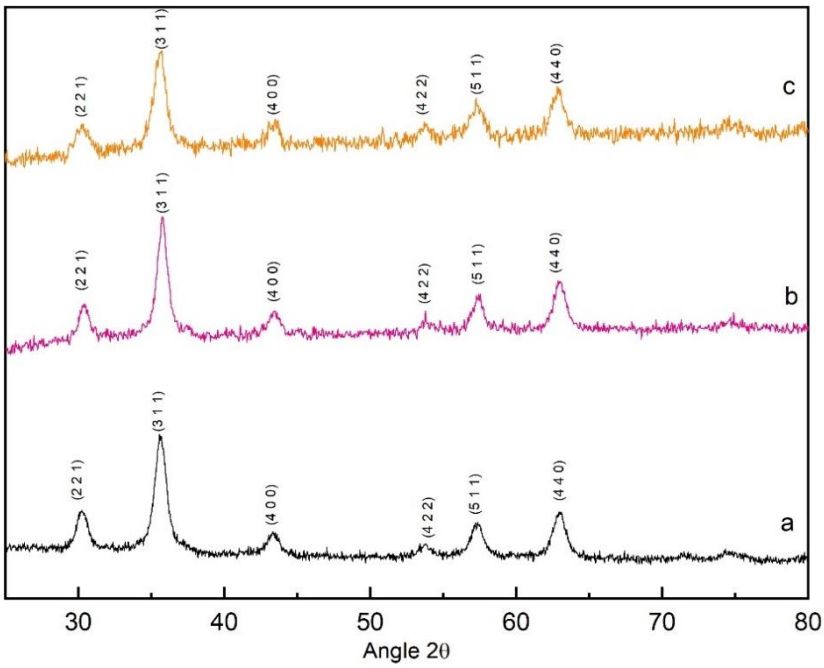

Figure 4.2: **X-ray pattern of iron oxide nanoparticles**. Naked NPs (a), DMSA coated NPs (b), APTES coated NPs (c).

TEM analysis was carried out to understand if the NPs coatings had any influence on the particle size. On Figure 4.3 A it is shown the non-coated NPs with an average particle size of 9.1 ± 0.1 nm and uniform distribution. This average particle size is con-

sistent with superparamagnetic behavior and below the critical size for biomedical applications (≤ 15 nm) [14]. This small particle size is also relevant for the enzymatic-like activity since, the minor the particle the greater the enzymatic-like activity [30]. Regarding the coated SPIONs, the DMSA ones exhibit a lower particle size compared to APTES and naked NPs however this is not a significant difference and therefore one can affirm that the presence of a stabilizer does not influence particle size. In general, the average size from TEM images is coherent with the average crystallite size calculated with XRD, which indicates that the crystallite size is approximately the same as the NPs size and thus confirms the existence of a single domain core.

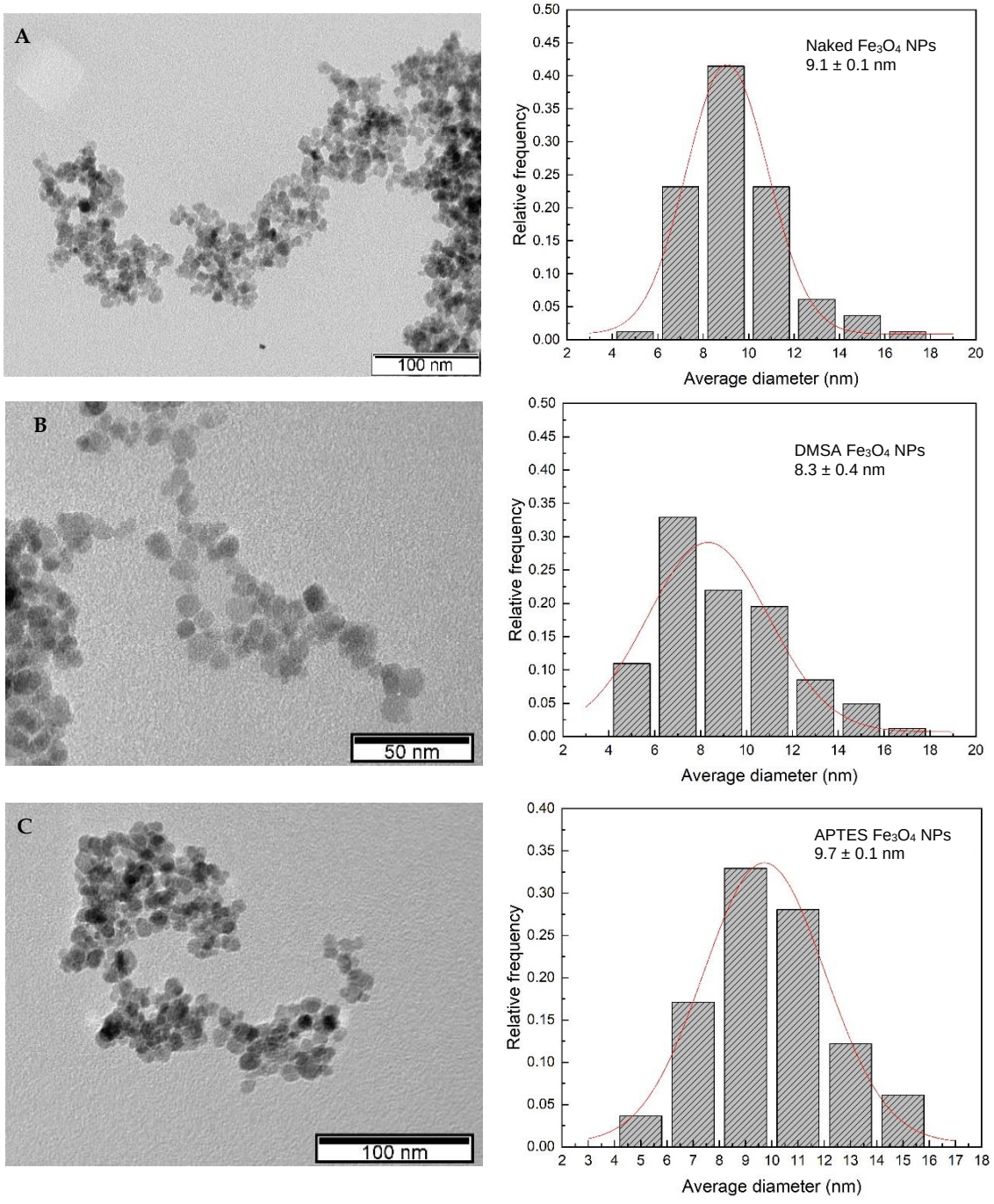

Figure 4.3: **TEM images and respective size distribution graph**. Naked NPs (a), DMSA coated NPs (b), APTES coated NPs (c).

Zeta potential was also assessed as indicator of the stability of the nanoparticles due to the electrostatic interactions. The nanoparticles are usually stable if the zeta potential is lower than -25 mV and higher than +25 mV. If not, the particles will have tendency to aggregate due to van der Waals interparticle attraction [11]. As so, SPIONs_APTES and SPIONs_DMSA were evaluated to understand the influence of the coatings in the NPs´ stability. Table 4.1 shows that SPIONs_APTES and SPIONs_DMSA have a zeta potential of 34 and -78 mV respectively when dispersed in water, which is in agreement with literature since, SPIONs_DMSA are negatively charge, due to the presence of an acid carboxylic terminal and SPIONs_APTES positively charge, because of the amine terminal at the NPs surface [38]. The same assay was done using McCoy culture media as the dispersion media instead of water and the NPs were incubated for 24h. The findings exhibit an alteration of the particle's charges and consequently in its stability, SPIONs_APTES have now a negative zeta potential of -0.27 mV and SPIONs_DMSA have a less negative zeta potential of -2.32 mV. This phenomenon is due to large amounts of proteins being adsorbed to the NPs, when in contact with the physiological environment which determines the average surface charge of the particle during incubation. A positively charged NP increases the quantity of proteins adsorbed to its surface due to electrostatic interactions since, typically, most proteins are negatively charged, leading to an alteration of zeta potential from positive to negative in cell culture medium. Regardless the particle charge when dispersed in McCoy media, the adsorbance of proteins is what dictates the SPIONs average surface charge [39]. This is confirmed since both SPIONs_APTES and SPIONs_DMSA present a negative zeta potential when dispersed in McCoy media.

Table 4.1**: Zeta potential and hydrodynamic size of SPIONS_APTES and SPIONs_DMSA in water and McCoy culture medium**. Zeta potencial; *Dh*, hydrodynamic size; PDI, polydispersity index. The SPIONs were incubated at 0.05 mg/ml in cell culture medium for 24 h.

Nanoparticle	Dispersion media	Zeta potencial (mV)	D_h (nm)	PDI
SPIONs_APTES	Water	35 ± 1	418 ± 5	0.33
	McCoy	-0.27 ± 2	28131 ± 4574	5.56
SPIONs_DMSA	Water	-80 ± 1	236 ± 4	0.25
	McCoy	-2.32 ± 3	22260 ± 1883	5.61

The hydrodynamic diameter of the NPs and how the absorbance of proteins affects it was also studied by DLS analysis. The hydrodynamic sizes displayed in Table 4.1 show SPIONs_APTES have a mean hydrodynamic diameter of 418 nm and SPIONs_DMSA 236 nm when dispersed in water. However, the average size significantly increases when the NPs are dispersed in culture medium, 22260 and 28131 nm for SPIONs_APTES and SPIONs_DMSA respectively, which confirms the absorbance of proteins at the surface of the NPs. It is not possible to make comparisons of dimensions obtained with DLS and other microscopic techniques (XDR and TEM), as DLS measures

the hydrodynamic diameter NPs takes into consideration the molecules at the NPs surfaces, contrarily to the size results obtained by TEM, that only measure the single iron core diameter of the NP.

4.2. Chemical enzymatic assays

One of the main objectives of this work is to study the enzymatic-like activity of the produced NPs. As a first approach, it was important to understand if the APTES and DMSA coated SPIONs had indeed the enzymatic-like activity. To do so, some basic visual tests were executed. In Figure 4.4 it is visible that for both types of SPIONs the TMB was catalyzed by NPs, generating the blue color, thus confirming the peroxidase-like activity of the synthesized NPs under acidic pH. The catalase-like activity of the NPs was also confirmed for APTES and DMSA through the bubbles that arose in both cuvettes due to the catalase reaction that converts H_2O_2 in O_2, at pH 7.4 [31].

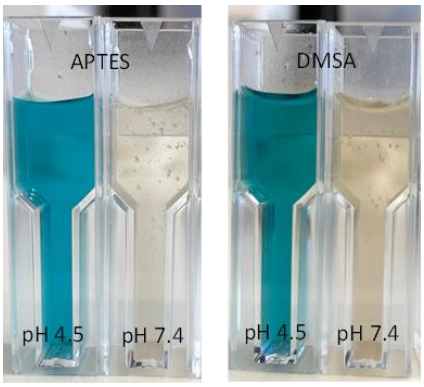

Figure 4.4: **Presence of peroxidase and catalase-like activities at pH 4.5 and 7.4.** APTES coated NPs possess both enzymatic-like activities (a), DMSA coated NPs possess both enzymatic-like activities (b).

4.2.1. pH assays

Considering the biomedical application of this work, it is essential to consider the cellular environment and how it affects the enzymatic-like activity. Regarding peroxidase-like activity, NPs require a pH between 3.5 and 6 to have a significant activity and in the cellular environment this type of pH levels is only found in lysosomes (pH 5.5) [40]. However, in the laboratory, it is only possible to manipulate cells with a pH around 7.4, any acidic pH would kill them. Nevertheless, peroxidase-like activity assays where SPIONs catalyze the reaction of the substrate TMB, since this activity mechanism must first form an intermediate complex with an appropriate substrate before catalysis can occur, in the presence of H_2O_2 producing a blue color with a maximum absorbance at 652 nm. The reaction was carried out with 10 µL of SPIONs (5 mg/ml), 25 µL of H_2O_2 (8.8 M), 100 µL of TMB (10 mg/mL) and 2 mL of phosphate buffer pH 5.5, during 3 min. In Figure 4.5, for pH 5.5 buffer solution, the NPs demonstrated intensive peroxidase-like activity, with an absorbance variation of 0.929 for DMSA SPIONs and 0.290 for SPIONs_APTES, proving this kind of enzymatic-like activity could occur in cells lysosomes.

The activity is more intense using DMSA_SPIONS as TMB yields a stronger affinity towards a negatively charged nanoparticle surface because of its two amine groups. For pH 7.4 we understand that the peroxidase-like activity demonstrated by APTES and DMSA stabilized SPIONs is not consistent, and it does not show a progressive increasement of the absorbance throughout the time period, that would be expected from a growth in the catalysis of TMB by the SPIONs. The same was verified for a pH of 7, thus it would not be a good substitute for cellular assays. Therefore, the peroxidase-like activity is not viable for cellular assays [41].

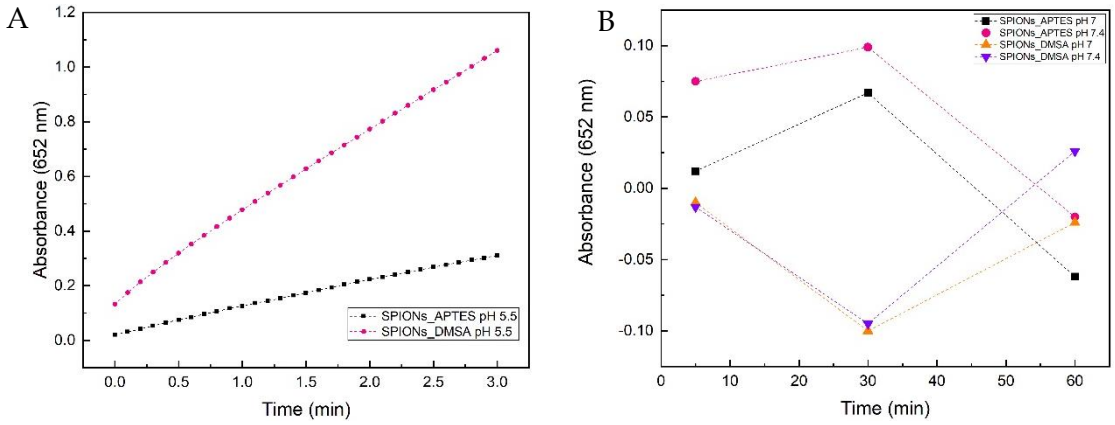

Figure 4.5: **pH depedence of peroxidase-like activity of APTES and DMSA coated SPIONs**. Peroxidase-like activity pH 5.5 (a), Peroxidase-like activity pH 7 and 7.4 (b).

Likewise, catalase-like activity is pH dependent and has its peak at a pH 7.4. This pH level is very favorable for cellular tests, and it is also a pH abundant in the cell environment, mainly in the cytosol. The catalase-like activity evaluates the reduction of hydrogen peroxide, as it is transformed into oxygen and the absorbance is measured at 240 nm, corresponding to the maximum absorbance of hydrogen peroxide. The reaction was carried out with 40 µL of SPIONs (0.5 mg/ml), 0.57 µL of H_2O_2 (8.8 M) (5 mM in the reaction medium), 100 µL and 1 mL of phosphate buffer solution with a pH 7.4, for 30 min. Figure 4.6 displays the results from those tests, and one can verify that DMSA coated SPIONs have a more considerable catalase-like activity with absorbance variation of 0.171 compared to 0.070 of SPIONs_APTES. SPIONs_DMSA showed activity higher than that of APTES since it presents a lower hydrodynamic diameter.

The same experiment was done using two different buffer solutions: PBS and McCoy culture medium to better mimetic the physiological natural environment. With this test (Figure 4.6 b) it was understood that the McCoy culture medium greatly affected the measurement and that the results were not feasible. One probable explanation for this is that cell culture mediums have more proteins and salts in its composition that adsorb to the NPs surface, which increased the SPIONs hydrodynamic diameter and thus decreasing the activity [39], [30].

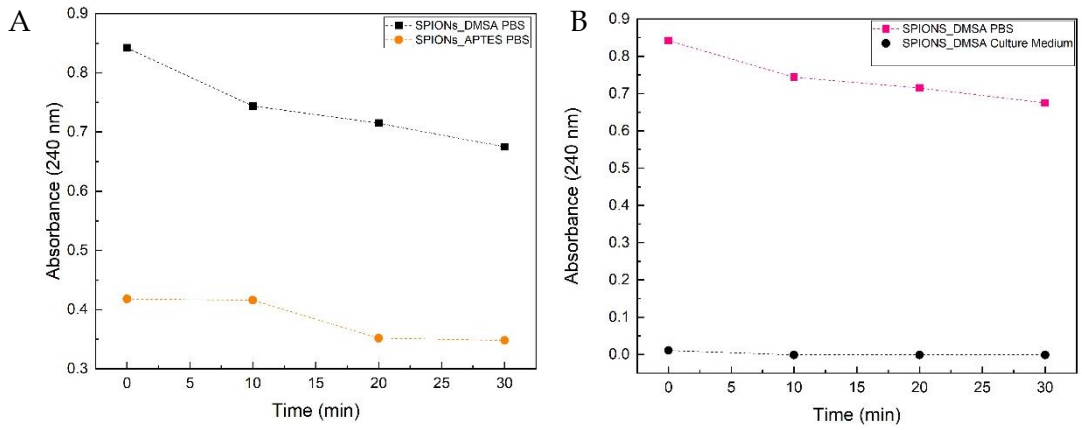

Figure 4.6: **Catalase-like activity of APTES and DMSA coated SPIONs**. Catalase-like activity PBS pH 7.4 (a); DMSA coated SPIONs catalase-like activity PBS pH 7.4 and McCoy culture medium pH 7.4 (b).

4.2.2 Hydrogen peroxide concentration dependence

Hydrogen peroxide is one of the main components of catalase-like activity, however it is a highly toxic one and the amounts formerly used would be severely cytotoxic for cells. Therefore, some additional tests were performed to see if the amount of hydrogen peroxide used could be lowered while maintaining the catalase-like activity. The quantities used were 2.58 µL of H_2O_2 diluted to 194 mM and 0.26 µL corresponding to 500 µM and 50 µM of H_2O_2 in the reaction medium, respectively the other variables were the same as before.

The results shown in Figure 4.7 demonstrate that for 500 µM of H_2O_2 the catalase-like activity is barely exhibited for either of the SPIONs being used and that, for 50 µM of H_2O_2 catalase-like activity is not existing. Thus, it is possible to conclude that relevant catalase-like activity is only possible with 5 mM H_2O_2 in the reaction medium, which could be destructive to cells.

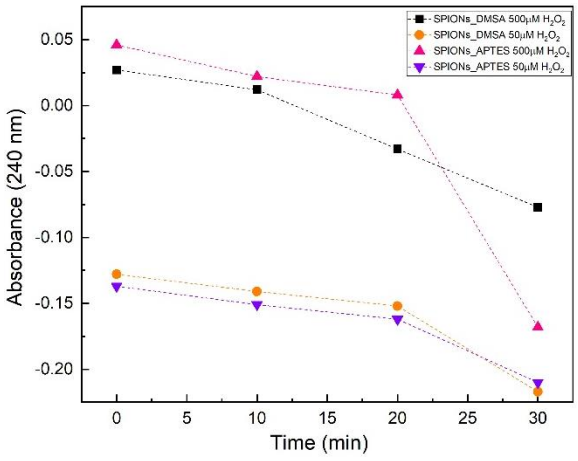

Figure 4.7: **Hydrogen peroxide concentration dependence catalase-like activity of APTES and DMSA coated SPIONs for 500 µM and 50 µM of H_2O_2.**

4.3. Cytotoxicity assays

In research work for a biomedical application, a very important stage is the cytotoxicity evaluation of the components. This study was performed using the SaOs-2 cell

line, an osteosarcoma cell line. The resazurin cytotoxicity test relies on the metabolic activity of living cells that reduce resazurin to resorufin, the reduction is visible due to a color change from dark blue to purple. Therefore, the conversion of resazurin to resorufin is proportional to the number of metabolically active cells (live cells). The results of the resazurin cell viability assay are expressed as percentage of viable cells in relation to the control: [% cell viability = NP treated cells/control cells x 100]. Control implies an untreated cell (without SPIONs) under the same condition as the rest of the samples.

The cytotoxicity assessment was performed for SPIONs with both coatings and for a wide range of NPs concentrations. With the results shown in Figure 4.8, it is possible to say that for NPs concentrations below 0.25 mg/mL the DMSA coated SPIONs do not cause a considerable cytotoxic effect, since a component is only considered to have a significant cytotoxic effect if the cell viability is less than 80%. This being said, DMSA stabilized SPOINs cause cytotoxicity in concentrations starting from 0.5 mg/mL, being significantly more severe at 1 and 2 mg/ml. When analyzing the results referent to APTES coated SPIONs, one can see that it does not possess a behavior similar to the DMSA`s, that increases its cytotoxicity with the increase of NPs concentration. From this assay, APTES coated NPs show cytotoxicity to the cells for all concentrations with a slight percentage difference between most concentrations.

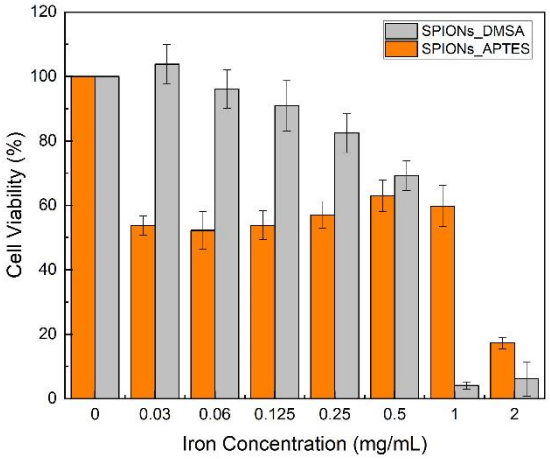

Figure 4.8: **SaOs-2 cell viability after 24 h incubation with DMSA and APTES coated SPIONs.** Data is expressed as average ± uncertainty for four replicas for each condition.

Considering the abnormal results obtained in the APTES cytotoxicity results from the resazurin assay, a different test was performed to validate the previous one. The resazurin assay relies in the reduction of resazurin to resofurin by live cells and the Live/Dead assay allows to count the exact number of live and dead cells based on microscopic images, instead of relying on the metabolic activity of the living cells. From Figure 4.9 one can affirm that the two assays are not consistent, and that Live/Dead reveals that the SPIONs_APTES are not cytotoxic for any concentrations, even for the higher ones. With both cytotoxicity assays, one can say that the concentration of 0.03 mg/mL of SPIONs, necessary for the catalase-like activity tests, is not cytotoxic for both coating agents, and thus can be used for *in vitro* catalase-like assays.

Following the assessment of SPIONs cytotoxicity, another crucial element to evaluate the enzymatic-like activity is the hydrogen peroxide and thus it is relevant to understand its toxicity levels to the cells. Since the catalase-like assay takes around 30 min and it is not very viable to take measurements in ten minutes intervals when performing cell-based tests, it was defined three times of incubation with a 30 min interval. As the cells were only going to be exposed to H_2O_2 during these time periods, the cytotoxicity assays were made for the same time intervals. The concentration of H_2O_2 that were studied correspond to the ones used during the chemical enzymatic tests and to 50 µM. Figure 4.10 a) confirms that these concentrations have a severe cytotoxic impact in the cells, killing all cells in the wells. The conclusion from this study is that the H_2O_2 amount required for the chemical catalase test is not fitting for cell assays. However, for 50 µM of H_2O_2, in Figure 4.10 b), the percentage of cell viability is much higher despite still being cytotoxic [42]. SPIONs were also used for the latter assay, at a concentration that was previously demonstrated to be not cytotoxic, so the cytotoxicity can only be due to the H_2O_2.

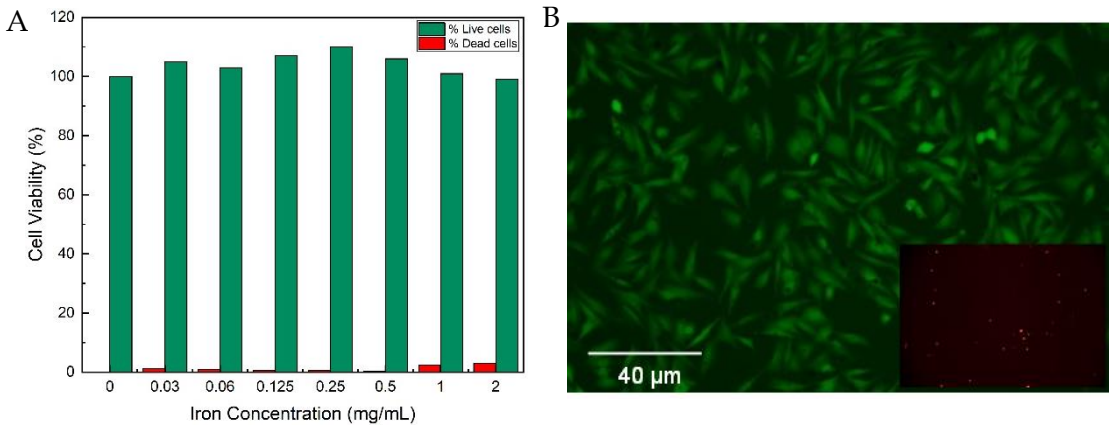

Figure 4.9: **SaOs-2 cell viability after 24 h incubation with SPIONs_APTES**. Data is expressed as average ± uncertainty for at least ten images for each condition. (a) Image from the epifluorescence microscopy live and dead cells 0,03 mg/mL SPIONs_APTES (b).

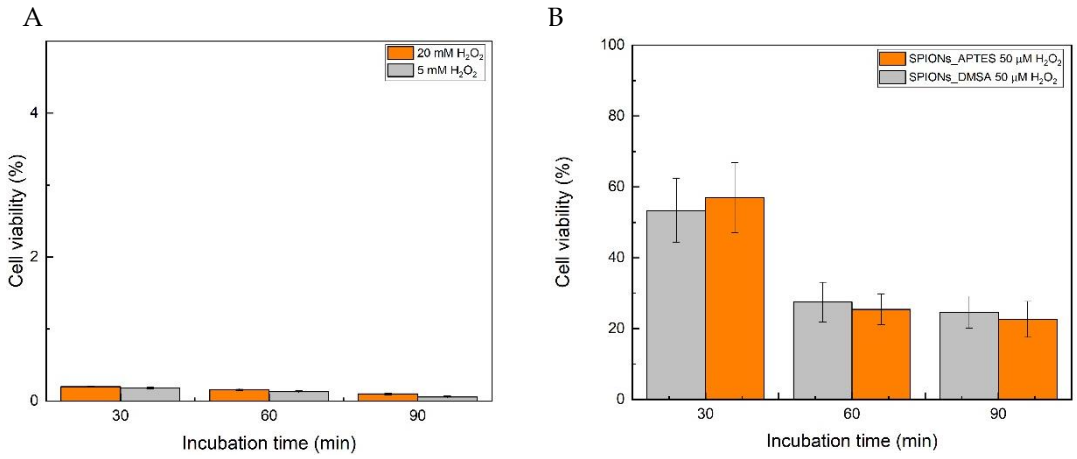

Figure 4.10: **SaOs-2 cell viability after incubation with H_2O_2.** Data is expressed as average ± uncertainty for at least four replicas for each condition. Cytotoxicity after 30, 60 and 90 min Incubation time with H_2O_2 20 and 5 mM (a). Cytotoxicity after 30, 60 and 90 min incubation time with H_2O_2 50µM + 0.03 mg/mL SPIONs (b).

4.4. Cellular uptake

4.4.1. Qualitative analysis with Prussian Blue staining

The SPIONs interaction with the SaOs-2 cell line was assessed using cell monolayer. Cells were exposed to SPIONs_DMSA and SPIONs_APTES for 1 h, 3 h, 6 h and 24 h. The SPIONs localization was identified with Prussian blue staining. Figure 4.11 shows the Prussian blue staining images of SPIONs localization after 1 h, 6 h and 24 h of exposure for SPIONs_DMSA and SPIONs_APTES, as well as the control of untreated cells. A qualitative analysis of the images indicates a rapid interaction of both types of SPIONs with the cell membrane. The higher predominance of blue for long periods of exposure is evidence of an increase of SPIONs either strongly attached to the cell membrane or already incorporated. Comparing both surfactants, after 6 h of exposure, the intracellular uptake of SPIONs_APTES was higher than for SPIONs_DMSA here, the APTES_SPIONs present themselves along the shape of the cells demonstrating their internalization. This evidence is only observed for the DMSA_SPIONs for a 16 h incubation time again, which, goes according to the literature describing a higher rate of internalization for NPs with a positive surface charge [38], [39], [43].

4.4.2. Quantitative analysis with 1,10-phenantroline colorimetric method

With the previous assay, one could say that, by the images obtained it was not certain that the NPs were internalized and that they were only adherent to the surface of the cell. So, we proceeded to quantitively determine the Fe content of the cells. To evaluate the SPIONs internalization in a quantitative way many techniques are in use, including ultraviolet spectrophotometry (UV-Vis) [44]. Colorimetric methods commonly employed for the quantitation of complexed iron in biological samples rely on an initial treatment, which releases the complexed iron for its subsequent quantitative determination [45]. For this reason, 1,10-phenantroline colorimetric method was used to determine the iron concentration in cultured cells [46],[47].

The qualitative iron uptake study can be confirmed by the quantitative analyses of intracellular iron uptake shown in Figure 4.12. This analysis was done for five different incubation times using both coated SPIONs with [NPs] of 0.03 mg/mL corresponding to a [Fe] of 0.021 mg/mL. It can be observed that after 6 hours of nanoparticles incubation, the concentration of absorbed iron is at its maximum for both NPs and that APTES coated SPIONs show a higher internalization than DMSA_SPIONs confirming a higher rate of internalization for NPs with a positive surface charge. The drastic decrease of [Fe] for 16 and 24 h can be justified by the reduction of cells in the plate wells, which was also previously observed.

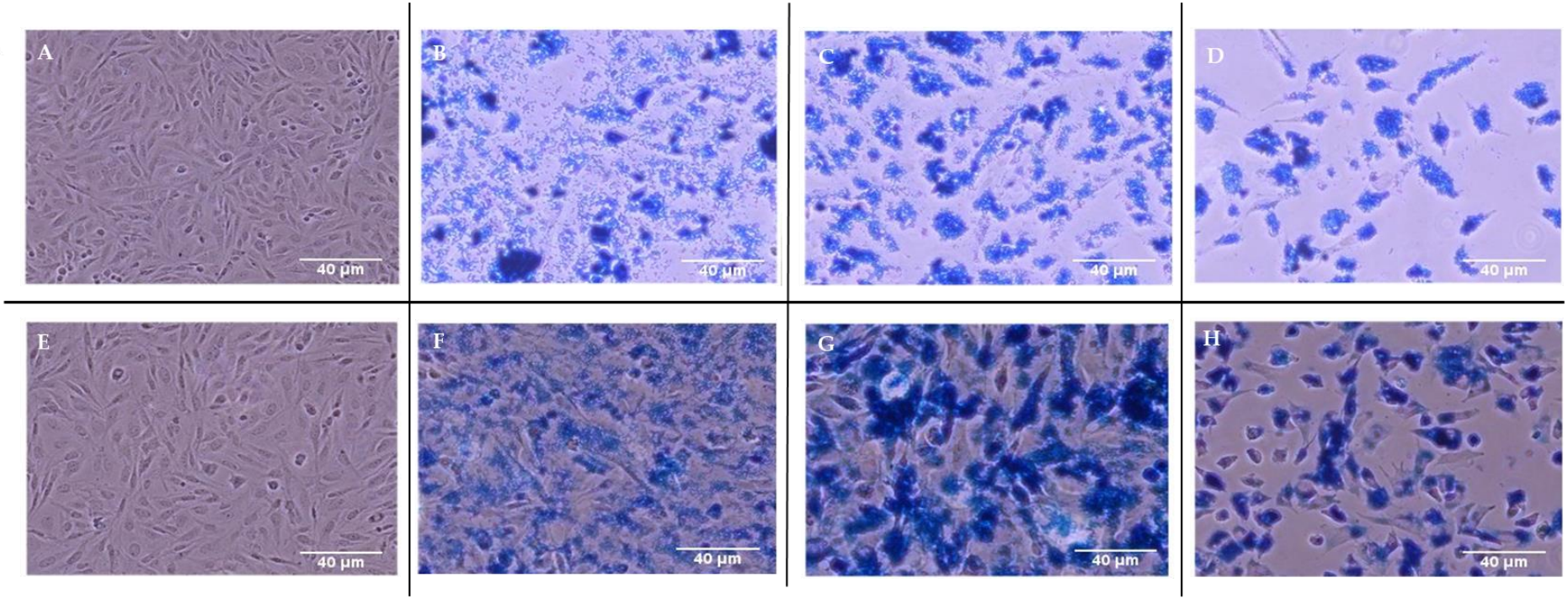

Figure 4.11: **Prussian blue staining of SPIONs intracellular localization in SaOs-2 cells incubated**. APTES_SPIONs (A-D), DMSA_SPIONs (E-H). Untreated cells (A, E) comparing with cells incubated with 0.03 mg/mL of SPIONs for 1 h (B, F) 6 h (C,G) and for 24 h (D,H). Bright field images with 20x objective magnification (A, B, C, G, H, I) with scale bar: 40 µm.

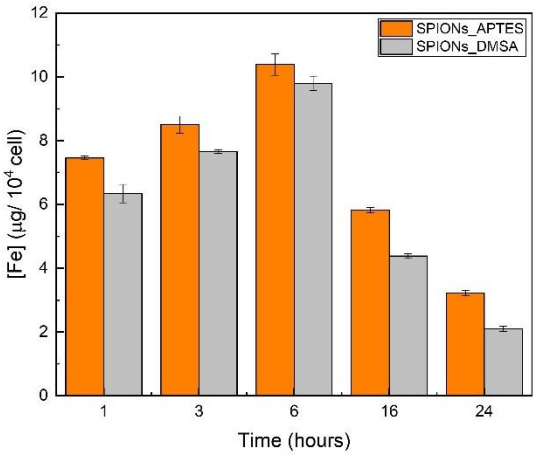

Figure 4.12: **Intracellular iron content quantification by 1,10-phenantroline colorimetric method**. The iron uptake is expressed as weight of iron per 1×10^4 cells and measured after 1 h, 3h, 6h, 16 h and 24 h of 0,03 mg/mL incubation of DMSA and APTES coated SPIONs. Data is expressed as average ± standard deviation for three replicas.

4.5. Intracellular catalase-like activity

The main goal of this work is to determine if the SPIONs enzymatic-like activity is observed intracellularly and to compare this activity in a normoxia and hypoxia environment that would simulate the tumor environment. There are several methods to evaluate the catalase-like activity, one of them being assessing the dissolved O_2 that should increase throughout a period of time, thus proving the existence of the activity [31]. Another approach was to replicate the enzymatic assay done before, this is, to measure the absorbance at 240 nm and see if the H_2O_2 was decreasing. To do so, once cell seeding and DMSA_SPIONs (0.03 mg/mL) internalization was done, H_2O_2 was added to the wells in a 5 mM concentration. After 1 h 30 min, 1 h and 30 min the supernatant was taken out and used to measure the residual H_2O_2. Ideally, the absorbance would diminish along the increasing time periods, indicating that cells were consuming the H_2O_2 present in the reaction medium and using it for the catalase-like reaction using SPIONs as the intermediate. By the results displayed in Table 4.2, it is possible to say that there is no apparent relation between the values that would indicate the catalase-like activity. With these time periods, the expected results were to have a much more obvious reduction in the absorbance, compared to the absorbance variation of 0.171 in the chemical assays, thus this approach was rejected.

Table 4.2: **Catalytic activity of IONzymes *in vitro*:** H_2O_2 absorbance at 240 nm after 0, 30, 60 and 90 min.

Time (min)	Absorbance (240 nm)	Absorbance control (240 nm)
0	0.245	0.245
30	0.339	0.315
60	0.268	0.284
90	0.322	0.290

Given these results, it was necessary to adopt another strategy. It was thought that Live/Dead assays could be a good option because using this method we would have the percentage of live and dead cells in a normoxia and hypoxia environment. In the hypoxia environment, the O_2 levels were reduced to the minimum possible (2%) and by comparing the results from both environments we would understand if there was a sufficient catalase-like reaction, these because in a hypoxia environment, does not promote cell growth, however with the catalase-like activity they would produce their own oxygen thus potentiating cellular growth. For this assay cells were incubated with 0.03 mg/mL of SPIONs_APTES and DMSA, and the amount of H_2O_2 was severely reduced to 50 μM as the amount previously used was cytotoxic and could also be influencing the results.

In Figure 4.13 we can observe that there is a clear difference among the control images and the ones from 1 h incubation with H_2O_2 regarding the background noise of the live cell's images. The 1 h incubation with H_2O_2 shows a green background, they are very dark which makes it almost impossible to count the cells. The problem here identified is that que calcein does not acquire its typical fluorescence and thus the images are poorest. A possible explanation for these is that some residual H_2O_2 reacts with calcein with makes this compound lose some of its fluorescent properties. This explanation comes from the fact that the control images are fine and the only different element between these and the other ones is the addition of H_2O_2. In closing, this approach was also discarded due to the poor image quality.

Once again, there was the need to find a new solution for this problem. Maintaining the same principle from the Live/Dead studies, resazurin assay was the most obvious solution. Hence, we proceeded with the resazurin studies using the same SPIONs concentration (0.03 mg/mL) and the 50 μM of H_2O_2 for same time periods (30 min, 1 h and 1 h 30 min), in a normoxia and hypoxia environment. The controls for this experiment were untreated cells (without SPIONs and H_2O_2) in both environments.

The results in Figure 4.14 show that in a hypoxia environment there is a reduction of viable cells either for APTES or DMSA SPIONs. This reduction of viable cells indicates that the catalase-like enzymatic activity was not sufficient for cells to survive. The low or inexistent catalase-like activity may be due to lack of H_2O_2 to start the reaction. This is, previously, in the chemical assays, we determined that with 50 μM of H_2O_2 there was no catalase-like activity but, nevertheless cells by their own produce H_2O_2 and there for it was thought that the combination of both amounts would be sufficient to produce enough O_2 for them to, at least, have a cell viability close to the one in a normoxia environment. Overall, the catalase-like activity is not exhibited intracellularly in the conditions that we used.

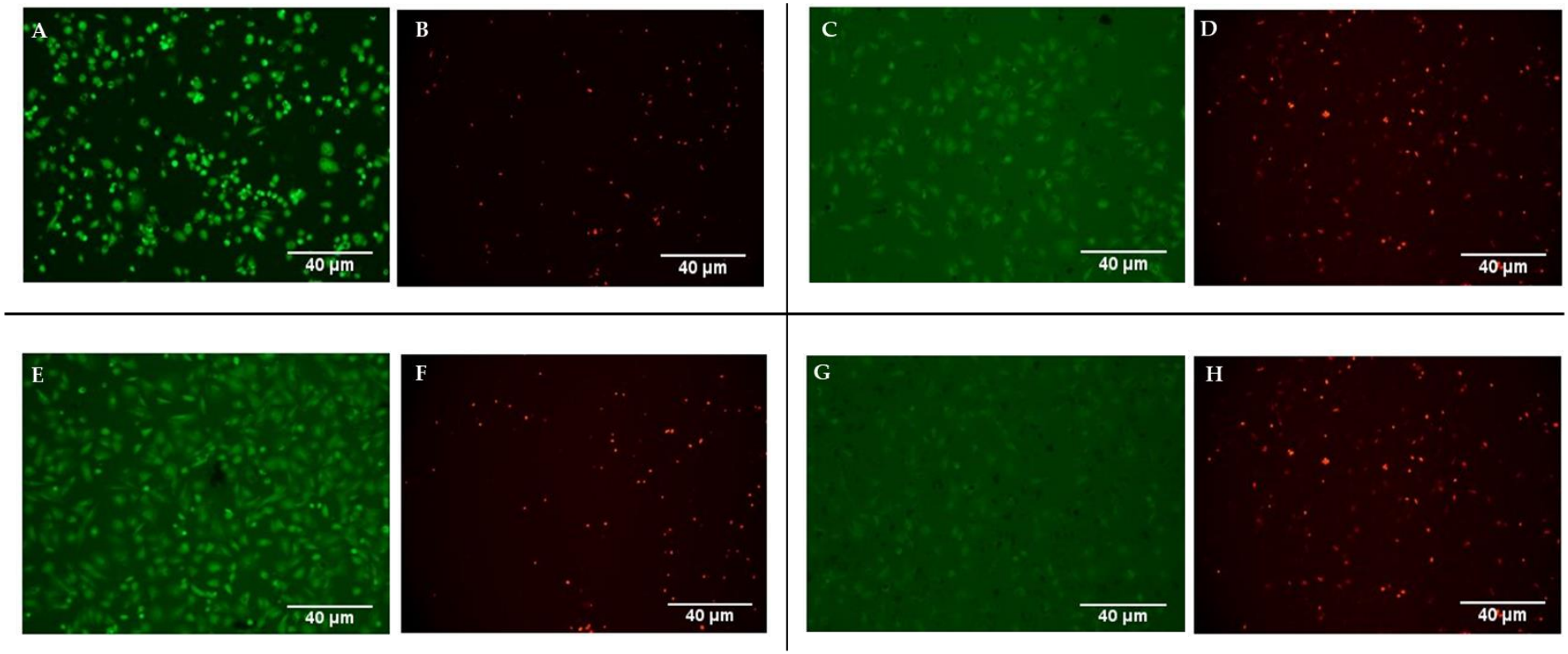

Figure 4.13: **Live/Dead images of SaOs-2 cells incubated with 0.03 mg/mL SPIONs**. APTES_SPIONs (A-D), DMSA_SPIONs (E-H). Untreated live cells (A, E) comparing with untreated dead cells (B, F). Cells incubated with 50 µM H_2O_2 for 1 h: live cells (C,G) comparing with dead cells (D, H). Epifluorescence microscopy images with 10x objective magnification (A, B, C, G, H, I) with scale bar: 40 µm.

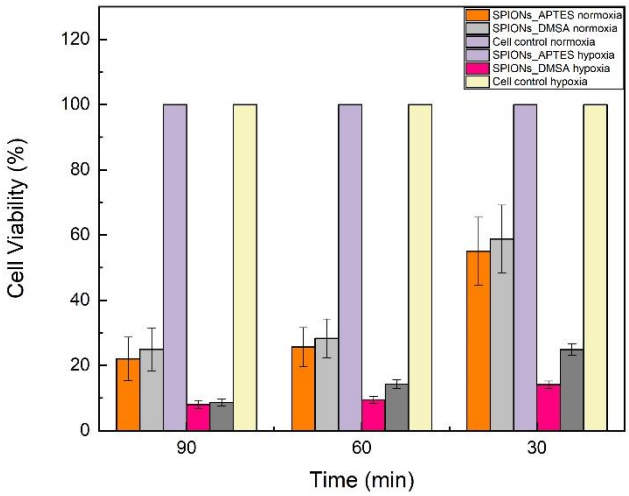

Figure 4.14: **SaOs-2 cell viability 0.03 mg/ml SPIONs after 30 min, 1 h and 1 h 30 min with H_2O_2 50µM incubation in normoxia and hypoxia**. Data is expressed as average ± uncertainty for at least five replicas for each condition.

4.6. Magnetic Hyperthermia

Magnetic hyperthermia treatment aims for cell death by increasing temperature in tumor cells. These cells are extremely sensitive to temperature and its death can be caused by apoptosis with temperatures between 40 and 44 °C [16], thus for experimental studies the focus is in increasing the NPs´ temperature by 5 °C which corresponds to temperature difference from 37 to 42 °C in the human body.

The heating of iron oxide magnetic nanoparticles in the presence of an alternating magnetic field is attributed to two-loss mechanisms: Brownian rotation and Néel relaxation of the particles' magnetization. When Fe_3O_4 NPs are in suspension, Brownian and Néel relaxations are present [48]. The Brownian relaxation involves the rotation of the particle itself against the forces coming from the solution, while Neél's relaxation is due to the rotation of the particle's magnetic moment to the equilibrium state, without implying the rotation of the particle itself [49]. Initially, five concentrations of NPs, like the ones used in previous assays, were submitted to an AMF for 10 minutes. Figure 4.15 shows the temperature variation of both types of coated SPIONs. The results reveal that SPIONs_APTES have the 5 °C temperature variation with a 0.25 mg/mL concentration of NPs, whilst SPIONs_DMSA only reach that temperature with a slightly higher concentration 0.5 mg/mL. APTES_SPIONs also present a greater temperature difference from concentration of 0.25 mg/mL.

Before performing *in vitro* magnetic hyperthermia assays, the influence of cell culture medium in the heating capacity of SPIONs was evaluated. SPIONs were dispersed in cell culture medium and left in the incubator for 4 h to simulate the cell environment. Magnetic hyperthermia assays were performed with the same conditions as before.

In a general manner, Figure 4.16 demonstrates that for both coatings there is no significant difference between the dispersion mediums and that the 5 °C temperature variation is reached at the same concentrations for either water or culture medium so, one can affirm that change of dispersion medium does not seriously influence the temperature variation of the NPs. However, it is also possible that the NPs were not in the incubator for long enough and

thus there was no time for total protein adsorption on the NPs surface, so the study does not demonstrate the complete influence of proteins. A possible justification for the constant variation of temperature among dispersion mediums is that the coating can entrap the iron oxide core, reducing the NPs mobility and consequently decreasing the contribution of the Brownian relaxation mechanism in the SPIONs heat dissipation.

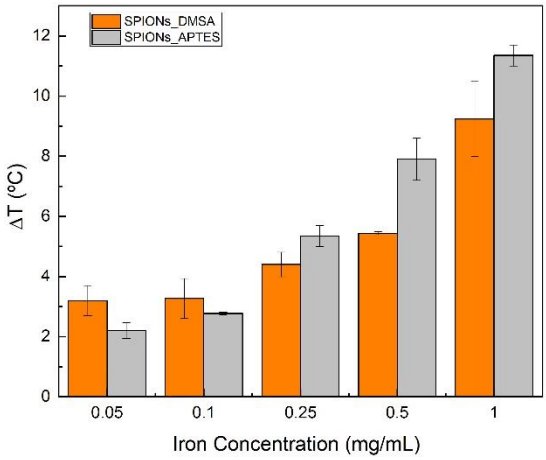

Figure 4.15: **Temperature variation per SPIONs concentration for both DMSA and APTES**. Temperature variation generated by an AMF application with intensity of 300 G at a frequency of 418.5 kHz, for 5 min. Data is expressed as average ± standard deviation for at least three measurements.

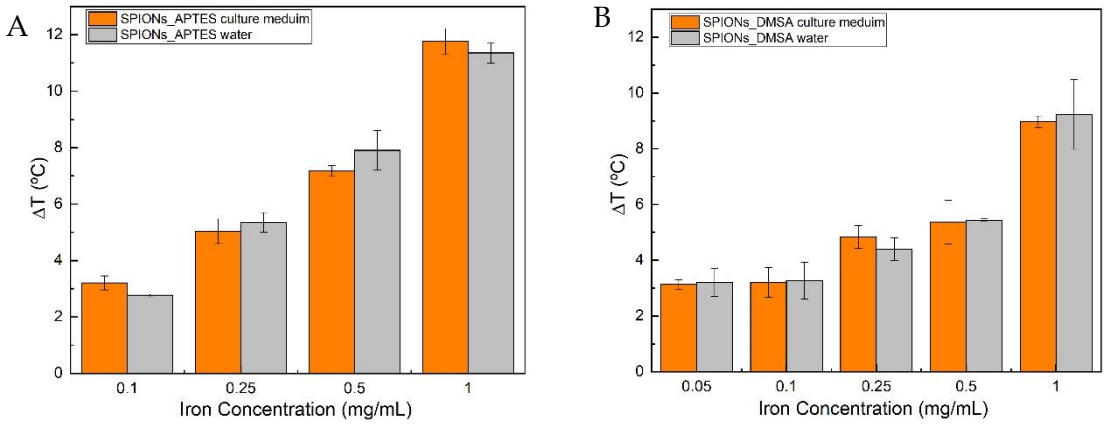

Figure 4.16: **Temperature variation per SPIONs concentration**. SPIONs_APTES dispersed in water and McCoy culture medium (a); SPIONs_DMSA dispersed in water and McCoy culture medium (b). Temperature variation generated by an AMF application with intensity of 300 G at a frequency of 418.5 kHz, for 5 min. Data is expressed as average± standard deviation for at least three measurements.

Given these results, a big problem is that the concentration of NPs needed to have the required temperature variation is higher than the one used for the catalase results and could be cytotoxic in the case of DMSA_SPIONs. These two assays, catalase-like activity and magnetic hyperthermia are not compatible in the sense that to have the 5 °C temperature variation is necessary to have a higher concentration of NPs however, for that same concentration of NPs to exhibit a good catalase-like activity a very high quantity of H_2O_2 is also needed. The amount of H_2O_2 would be very cytotoxic, as previously stated, therefore the assay would not be viable.

Further magnetic hyperthermia assays *in vitro* were intended nevertheless, these were not possible due to an equipment malfunction. The foreseeable results were that the temperature variation would decrease due to the NPs entrapment in the cells, which would decrease even more the Brownian relaxation mechanism therefore, heat generation could only be attributed to Néel relaxation [50]. Then, a comparison of cell viability before and after magnetic hyperthermia would be made to understand if indeed the cell viability would be reduced due to cell apoptosis a result of the temperature augmentation.

5. CONCLUSION AND FUTURE PERSPECTIVES

The main goal of this research work was to use SPIONs´ catalase and peroxidase-like activity and combine it with magnetic hyperthermia for cancer treatment.

SPIONs were used due to their unique properties, such as their biocompatibility and their ability to generate heat when subjected to a magnetic field as well as due to their newly found peroxidase-like and catalase-like activity. They were produced using the chemical co-precipitation method. Due to their low stability in aqueous suspension, SPIONs were coated with APTES and DMSA. The synthesized APTES_SPIONs, DMSA_SPIONs and naked SPIONs were characterized by FTIR, XRD, TEM and DLS analysis. By FTIR it was possible to observe characteristic bands of functional groups of both coatings, proving that the surface modification was successful. XRD analysis confirmed that the nanoparticles coated with APTES and DMSA maintained the crystalline structure of the naked nanoparticles. TEM images demonstrated that naked and coated the nanoparticles had a similar average NP size. Furthermore, the size obtained through TEM analysis is coherent with the average crystallite size calculated with XRD (8 to 9 nm). Zeta potential assays were performed to understand the influence of the stabilizing agents in the charge of the surface of the modified nanoparticles. Zeta potential measures revealed that both coatings confer stability in an aqueous medium to the nanoparticles. However, when dispersed in McCoy medium both types of SPIONs suffer from protein adsorption on the surface of the NP and that is what dictates the SPIONs average surface charge.

Following SPIONs characterization it was important to assess their enzymatic-like activities. For peroxidase-like activity, the assays were carried out using TMB as a substrate. The pH dependence of this activity was evaluated for pH 5.5, 7 and 7.4 to better mimic the intracellular environment of lysosomes and the cytosol. It was determined that DMSA and APTES coated SPIONs exhibit peroxidase-like activity using a buffer with pH 5.5, whereas the latter presented a lower peroxidase-like activity due to its surface positive charge. Regarding the neutral pH, none of the coated SPIONs presented a significant activity thus, it was concluded that peroxidase-like activity could not be assessed *in vitro*, as the pH that it requires would kill the cells. The catalase-like activity assays were assessed at 240 nm measuring the decomposition of hydrogen peroxide. For this assay, the activity was measured using PBS and McCoy medium culture at pH 7.4. Both coated SPIONs presented catalase-like activity, but DMSA coated nanoparticles showed higher activity than APTES since it presents a lower hydrodynamic diameter. Concerning the comparison between dispersion media, the results showed that the cell culture medium interfered with the activity due to having more proteins and salts in its composition that could adhere to the NPs surface, which would increase the SPIONs hydrodynamic diameter and thus decrease the activity. For the catalase-like activity it was also studied the hydrogen peroxide dependence, as this is a highly toxic compound

that could kill cells during *in vitro* tests, to this end two lower hydrogen peroxide concentrations were tested: 500 μM and 50 μM. The results demonstrated that for 500 μM of H_2O_2 the catalase-like activity is barely exhibited for both SPIONs being used and that, for 50 μM of H_2O_2 catalase-like activity does not exist.

Before assessing the catalase-like activity *in vitro*, a cytotoxicity assay was performed to confirm if SPIONs and H_2O_2 caused severe cytotoxic effects after 24 h incubation in SaOs-2 cells. Regarding SPIONs, the results showed that the concentration of 0.03 mg/mL of SPIONs, necessary for the catalase-like activity tests, is not cytotoxic for either coating and thus can be used for *in vitro* catalase-like assays. However, H_2O_2 demonstrated severe cytotoxicity for the higher concentrations (20 and 5 mM) and less toxicity with 50 μM. Further on, to confirm SPIONs internalization in SaOs-2 cells Prussian blue staining for qualitative analysis and 1,10-phenantroline colorimetric tests were done. Prussian blue staining images revealed that SPIONs present themselves along the shape of the cells demonstrating their internalization and that SPIONs coated with APTES have a quicker interaction then DMSA_SPIONs. 1,10-phenantroline colorimetric showed that there was iron content in the cells after only 1 h of incubation, proving that SPIONs do internalize.

The main objective of assessing catalase-like activity *in vitro* showed that in a hypoxia environment there is a reduction of viable cells for both APTES or DMSA SPIONs. This reduction of viable cells indicates that the catalase-like enzymatic activity was not sufficient for cells to survive. The low or inexistent catalase-like activity may be due to lack of H_2O_2 to start the reaction. This is, previously, in the chemical assays, we determined that with 50 μM of H_2O_2 there was no catalase-like activity but, nevertheless cells by their own produce H_2O_2 and therefor it was thought that the combination of both amounts would be sufficient to produce enough O_2 for them to, at least, have a cell viability close to the one in a normoxia environment. Overall, the catalase-like activity is not exhibited intracellularly in the conditions that we used.

Lastly, magnetic hyperthermia assays showed that SPIONs can achieve the temperature difference of 5 ^{o}C for SPIONs concentrations above 0.025 mg/mL with indicate that they can reach 42 ^{o}C, the theoretical temperature of the tumor cells that enter the apoptotic phase.

An important step would be to evaluate the expression of HIF (hypoxia-inducible factor) in normoxia and hypoxia conditions to assess that the SPIONs can reduce hypoxia present in the TME and then be used as a magnetic hyperthermia agent.

To assess the therapy's effectiveness, future work should be done using agar phantoms to mimic when SPIONs are injected in the body or directly into the tissue, tumor cells take up the SPIONs and stay fixed. These tests should then be compared to *in vitro* magnetic hyperthermia to better assess the effects of no Brownian relaxation. Also, cell viability assay should be performed following magnetic hyperthermia to detect levels of cell apoptosis.

As in this work only therapeutic features were considered, it would be valuable to also study more in depth the diagnosis features of SPIONs for MRI purposes so that the theranostics system would be fully assessed.

REFERENCES

[1] F. Bray, J. Ferlay, I. Soerjomataram, R. L. Siegel, L. A. Torre, and A. Jemal, "Global cancer statistics 2018: GLOBOCAN estimates of incidence and mortality worldwide for 36 cancers in 185 countries," *CA. Cancer J. Clin.*, vol. 68, no. 6, pp. 394–424, 2018, doi: 10.3322/caac.21492.

[2] X. Chen and S. T. Wong, "Cancer theranostics", in Cancer Theranostics, Elsevier, 2014, pp. 3–8. doi: 10.1016/b978-0-12-407722-5.00001-3.

[3] M. Ferreira, J. Sousa, A. Pais, and C. Vitorino, "The role of magnetic nanoparticles in cancer nanotheranostics," *Materials (Basel).*, vol. 13, no. 2, pp. 1–25, 2020, doi: 10.3390/ma13020266.

[4] L. Gao *et al.*, "Intrinsic peroxidase-like activity of ferromagnetic nanoparticles," *Nat. Nanotechnol.*, vol. 2, no. 9, pp. 577–583, 2007, doi: 10.1038/nnano.2007.260.

[5] T. Y. Yen *et al.*, "Catalase-Functionalized Iron Oxide Nanoparticles Reverse Hypoxia-Induced Chemotherapeutic Resistance," *Adv. Healthc. Mater.*, vol. 8, no. 20, pp. 1–8, 2019, doi: 10.1002/adhm.201900826.

[6] P. M. Crapo, T. W. Gilbert, and S. F. Badylak, "An overview of tissue and whole organ decellularization processes," *Biomaterials*, vol. 32, no. 12, pp. 3233–3243, 2011, doi: 10.1016/j.biomaterials.2011.01.057.

[7] F. R. Balkwill, M. Capasso, and T. Hagemann, "The tumor microenvironment at a glance," *J. Cell Sci.*, vol. 125, no. 23, pp. 5591–5596, 2012, doi: 10.1242/jcs.116392.

[8] C. Lennicke, J. Rahn, R. Lichtenfels, L. A. Wessjohann, and B. Seliger, "Hydrogen peroxide - Production, fate and role in redox signaling of tumor cells," *Cell Commun. Signal.*, vol. 13, no. 1, pp. 1–19, 2015, doi: 10.1186/s12964-015-0118-6.

[9] M. Z. Zou *et al.*, "Advances in nanomaterials for treatment of hypoxic tumor," *Natl. Sci. Rev.*, vol. 8, no. 2, 2021, doi: 10.1093/nsr/nwaa160.

[10] P. I.P. Soares, I. M.M. Ferreira, R. A.G.B.N. Igreja, C. M.M. Novo, and J. P.M.R. Borges, "Application of Hyperthermia for Cancer Treatment: Recent Patents Review," *Recent Pat. Anticancer. Drug Discov.*, vol. 7, no. 1, pp. 64–73, 2011, doi: 10.2174/157489212798358038.

[11] M. Mahmoudi, S. Sant, B. Wang, S. Laurent, and T. Sen, "Superparamagnetic iron oxide nanoparticles (SPIONs): Development, surface modification and applications in chemotherapy," *Adv. Drug Deliv. Rev.*, vol. 63, no. 1–2, pp. 24–46, 2011, doi: 10.1016/j.addr.2010.05.006.

[12] K. Hervé *et al.*, "The development of stable aqueous suspensions of PEGylated SPIONs for biomedical applications," *Nanotechnology*, vol. 19, no. 46, 2008, doi: 10.1088/0957-4484/19/46/465608.

[13] C. Sun, J. S. H. Lee, and M. Zhang, "Magnetic nanoparticles in MR imaging and drug delivery," *Adv. Drug Deliv. Rev.*, vol. 60, no. 11, pp. 1252–1265, 2008, doi: 10.1016/j.addr.2008.03.018.

[14] A. M. G. C. Dias, A. Hussain, A. S. Marcos, and A. C. A. Roque, "A biotechnological perspective on the application of iron oxide magnetic colloids modified with polysaccharides," *Biotechnol. Adv.*, vol. 29, no. 1, pp. 142–155, 2011, doi:

10.1016/j.biotechadv.2010.10.003.

[15] G. F. Goya, T. S. Berquó, F. C. Fonseca, and M. P. Morales, "Static and dynamic magnetic properties of spherical magnetite nanoparticles," *J. Appl. Phys.*, vol. 94, no. 5, pp. 3520–3528, 2003, doi: 10.1063/1.1599959.

[16] V. F. Cardoso, A. Francesko, C. Ribeiro, M. Bañobre-López, P. Martins, and S. Lanceros-Mendez, "Advances in Magnetic Nanoparticles for Biomedical Applications," *Adv. Healthc. Mater.*, vol. 7, no. 5, pp. 1–35, 2018, doi: 10.1002/adhm.201700845.

[17] J. Carrey, B. Mehdaoui, and M. Respaud, "Simple models for dynamic hysteresis loop calculations of magnetic single-domain nanoparticles: Application to magnetic hyperthermia optimization," *J. Appl. Phys.*, vol. 109, no. 8, 2011, doi: 10.1063/1.3551582.

[18] C. Glorieux, N. Dejeans, B. Sid, R. Beck, P. B. Calderon, and J. Verrax, "Catalase overexpression in mammary cancer cells leads to a less aggressive phenotype and an altered response to chemotherapy," *Biochem. Pharmacol.*, vol. 82, no. 10, pp. 1384–1390, 2011, doi: 10.1016/j.bcp.2011.06.007.

[19] J. Liu *et al.*, "Redox regulation of pancreatic cancer cell growth: Role of glutathione peroxidase in the suppression of the malignant phenotype," *Hum. Gene Ther.*, vol. 15, no. 3, pp. 239–250, 2004, doi: 10.1089/104303404322886093.

[20] M. Nita and A. Grzybowski, "The Role of the Reactive Oxygen Species and Oxidative Stress in the Pathomechanism of the Age-Related Ocular Diseases and Other Pathologies of the Anterior and Posterior Eye Segments in Adults," *Oxid. Med. Cell. Longev.*, vol. 2016, 2016, doi: 10.1155/2016/3164734.

[21] W. He, W. Wamer, Q. Xia, J. J. Yin, and P. P. Fu, "Enzyme-like activity of nanomaterials," *J. Environ. Sci. Heal. - Part C Environ. Carcinog. Ecotoxicol. Rev.*, vol. 32, no. 2, pp. 186–211, 2014, doi: 10.1080/10590501.2014.907462.

[22] S. Kumari, A. K. Badana, G. Murali Mohan, G. Shailender, and R. R. Malla, "Reactive Oxygen Species: A Key Constituent in Cancer Survival," *Biomark. Insights*, vol. 13, 2018, doi: 10.1177/1177271918755391.

[23] C. Shi *et al.*, "Catalase-based liposomal for reversing immunosuppressive tumor microenvironment and enhanced cancer chemo-photodynamic therapy," *Biomaterials*, vol. 233, p. 119755, 2020, doi: 10.1016/j.biomaterials.2020.119755.

[24] S. Singh, "Nanomaterials exhibiting enzyme-like properties (Nanozymes): Current advances and future perspectives," *Front. Chem.*, vol. 7, no. FEB, pp. 1–10, 2019, doi: 10.3389/fchem.2019.00046.

[25] L. Gao, K. Fan, and X. Yan, "Iron oxide nanozyme: A multifunctional enzyme mimetic for biomedical applications," *Theranostics*, vol. 7, no. 13, pp. 3207–3227, 2017, doi: 10.7150/thno.19738.

[26] N. Wang, L. Zhu, D. Wang, M. Wang, Z. Lin, and H. Tang, "Sono-assisted preparation of highly-efficient peroxidase-like Fe3O4 magnetic nanoparticles for catalytic removal of organic pollutants with H2O2," *Ultrason. Sonochem.*, vol. 17, no. 3, pp. 526–533, 2010, doi: 10.1016/j.ultsonch.2009.11.001.

[27] I. Bertini, H. B. Gray, and J. Stephen, LibreTexts, Catalase and Peroxidase. [Online]. Available: https://chem.libretexts. org/@go/page/60954

[28] N. V. S. Vallabani and S. Singh, "Recent advances and future prospects of iron oxide nanoparticles in biomedicine and diagnostics," *3 Biotech*, vol. 8, no. 6, p. 0, 2018, doi:

10.1007/s13205-018-1286-z.

[29] S. Liu, F. Lu, R. Xing, and J. J. Zhu, "Structural effects of fe3O4 nanocrystals on peroxidase-like activity," *Chem. - A Eur. J.*, vol. 17, no. 2, pp. 620–625, 2011, doi: 10.1002/chem.201001789.

[30] F. F. Peng, Y. Zhang, and N. Gu, "Size-dependent peroxidase-like catalytic activity of Fe3O4 nanoparticles," *Chinese Chem. Lett.*, vol. 19, no. 6, pp. 730–733, 2008, doi: 10.1016/j.cclet.2008.03.021.

[31] Z. Chen *et al.*, "Dual enzyme-like activities of iron oxide nanoparticles and their implication for diminishing cytotoxicity," *ACS Nano*, vol. 6, no. 5, pp. 4001–4012, 2012, doi: 10.1021/nn300291r.

[32] M. Li *et al.*, "State-of-the-art iron-based nanozymes for biocatalytic tumor therapy," *Nanoscale Horizons*, vol. 5, no. 2, pp. 202–217, 2020, doi: 10.1039/c9nh00577c.

[33] S. Gao, H. Lin, H. Zhang, H. Yao, Y. Chen, and J. Shi, "Nanocatalytic Tumor Therapy by Biomimetic Dual Inorganic Nanozyme-Catalyzed Cascade Reaction," *Advanced Science*, vol. 6, no. 3. 2019, doi: 10.1002/advs.201801733.

[34] P. I. P. Soares *et al.*, "Effects of surfactants on the magnetic properties of iron oxide colloids," *J. Colloid Interface Sci.*, vol. 419, pp. 46–51, 2014, doi: 10.1016/j.jcis.2013.12.045.

[35] S. I. C. J. Palma, M. Marciello, A. Carvalho, S. Veintemillas-Verdaguer, M. del P. Morales, and A. C. A. Roque, "Effects of phase transfer ligands on monodisperse iron oxide magnetic nanoparticles," *J. Colloid Interface Sci.*, vol. 437, pp. 147–155, 2015, doi: 10.1016/j.jcis.2014.09.019.

[36] A. Bayat, M. Shakourian-Fard, N. Ehyaei, and M. M. Hashemi, "A magnetic supported iron complex for selective oxidation of sulfides to sulfoxides using 30% hydrogen peroxide at room temperature," *RSC Adv.*, vol. 4, no. 83, pp. 44274–44281, 2014, doi: 10.1039/c4ra07356h.

[37] P. I. P. Soares *et al.*, "Thermal and magnetic properties of iron oxide colloids: Influence of surfactants," *Nanotechnology*, vol. 26, no. 42, 2015, doi: 10.1088/0957-4484/26/42/425704.

[38] M. Calero *et al.*, "Efficient and safe internalization of magnetic iron oxide nanoparticles: Two fundamental requirements for biomedical applications," *Nanomedicine Nanotechnology, Biol. Med.*, vol. 10, no. 4, pp. 733–743, 2014, doi: 10.1016/j.nano.2013.11.010.

[39] M. P. Calatayud, B. Sanz, V. Raffa, C. Riggio, M. R. Ibarra, and G. F. Goya, "The effect of surface charge of functionalized Fe3O4 nanoparticles on protein adsorption and cell uptake," *Biomaterials*, vol. 35, no. 24, pp. 6389–6399, 2014, doi: 10.1016/j.biomaterials.2014.04.009.

[40] D. E. Johnson, P. Ostrowski, V. Jaumouillé, and S. Grinstein, "The position of lysosomes within the cell determines their luminal pH," *J. Cell Biol.*, vol. 212, no. 6, pp. 677–692, 2016, doi: 10.1083/jcb.201507112.

[41] T. Matsubara, G. R. DiResta, S. Kakunaga, D. Li, and J. H. Healey, "Additive influence of extracellular pH, oxygen tension, and pressure on invasiveness and survival of human osteosarcoma cells," *Front. Oncol.*, vol. 3 JUL, no. July, pp. 1–15, 2013, doi: 10.3389/fonc.2013.00199.

[42] K. Reznikov *et al.*, "Clustering of apoptotic cells via bystander killing by peroxides,"

FASEB J., vol. 14, no. 12, pp. 1754–1764, 2000, doi: 10.1096/fj.99-0890com.

[43] D. Zhang, L. Wei, M. Zhong, L. Xiao, H. W. Li, and J. Wang, "The morphology and surface charge-dependent cellular uptake efficiency of upconversion nanostructures revealed by single-particle optical microscopy," *Chem. Sci.*, vol. 9, no. 23, pp. 5260–5269, 2018, doi: 10.1039/c8sc01828f.

[44] S. Liao, C. Liu, F. Lin, and K. C. Wu, "Functionalized magnetic iron oxide / alginate core- shell nanoparticles for targeting hyperthermia," pp. 3315–3328, 2015.

[45] W. W. fish, "Rapid Colorimetric Micromethod for the Quantitation of Complexed Iron in Biological Samples," *Methods Enzymol.*, vol. 158, no. C, pp. 357–364, 1988, doi: 10.1016/0076-6879(88)58067-9.

[46] M. M. Yallapu, S. F. Othman, E. T. Curtis, B. K. Gupta, M. Jaggi, and S. C. Chauhan, "Multi-functional magnetic nanoparticles for magnetic resonance imaging and cancer therapy," *Biomaterials*, vol. 32, no. 7, pp. 1890–1905, 2011, doi: 10.1016/j.biomaterials.2010.11.028.

[47] M. M. Yallapu, S. P. Foy, T. K. Jain, and V. Labhasetwar, "PEG-functionalized magnetic nanoparticles for drug delivery and magnetic resonance imaging applications," *Pharm. Res.*, vol. 27, no. 11, pp. 2283–2295, 2010, doi: 10.1007/s11095-010-0260-1.

[48] G. Kandasamy and D. Maity, "Recent advances in superparamagnetic iron oxide nanoparticles (SPIONs) for in vitro and in vivo cancer nanotheranostics," *Int. J. Pharm.*, vol. 496, no. 2, pp. 191–218, 2015, doi: 10.1016/j.ijpharm.2015.10.058.

[49] Y. H. Chen, C. H. Cheng, W. J. Chang, Y. C. Lin, F. H. Lin, and J. C. Lin, "Studies of magnetic alginate-based electrospun matrices crosslinked with different methods for potential hyperthermia treatment," *Mater. Sci. Eng. C*, vol. 62, pp. 338–349, 2016, doi: 10.1016/j.msec.2016.01.070.

[50] S. Dutz and R. Hergt, "Magnetic nanoparticle heating and heat transfer on a microscale: Basic principles, realities and physical limitations of hyperthermia for tumour therapy," *Int. J. Hyperth.*, vol. 29, no. 8, pp. 790–800, 2013, doi: 10.3109/02656736.2013.822993.

[51] B. Azadbakht, H. Afarideh, M. Ghannadi-Maragheh, A. Bahrami-Samani, and M. Asgari, "Preparation and evaluation of APTES-PEG coated iron oxide nanoparticles conjugated to rhenium-188 labeled rituximab," *Nucl. Med. Biol.*, vol. 48, pp. 26–30, 2017, doi: 10.1016/j.nucmedbio.2016.05.002.

[52] N. Fauconnier, J. N. Pons, J. Roger, and A. Bee, "Thiolation of maghemite nanoparticles by dimercaptosuccinic acid," *J. Colloid Interface Sci.*, vol. 194, no. 2, pp. 427–433, 1997, doi: 10.1006/jcis.1997.5125.

[53] M. Talelli *et al.*, "Superparamagnetic iron oxide nanoparticles encapsulated in biodegradable thermosensitive polymeric micelles: Toward a targeted nanomedicine suitable for image-guided drug delivery," *Langmuir*, vol. 25, no. 4, pp. 2060–2067, 2009, doi: 10.1021/la8036499.

A.

SPIONs stabilization with APTES and DMSA

The procedure followed for stabilizing SPIONS with 3-aminopropyltriethoxysilane (APTES) is as follows: APTES (Merck) 10% (v/v) solution was made and then added to the nanoparticles already produced along with of glycerol glycerol in a 1:2 ratio. Afterwards the mixture was left to react inside the hood for 2h at 90º C under mechanical stirring with a nitrogen atmosphere. Past the 2 h and after cooling the solution to room temperature, the NPs were separated from the supernatant and washed 4 times with Millipore water alternated with ethanol [51].

For stabilizing with dimercaptosuccinic acid (DMSA) the following steps were done: Before coating the previously produced SPIONs with it is necessary to adjust the pH of the solution to 3 with nitric acid 65% (Merck). 0.3 M DMSA (*Sigma-Aldrich*) was then added immediately at a 4 ratio of [DMSA]/[Fe^{2+}] [52]. DMSA was dissolved in 5 mL of Millipore water and the pH was adjusted to 5.5 using 0.1 M NaOH (CARLO ERBA Reagents) under magnetic stirring. The reaction was performed in an ultrasound bath for 3 h. After this time, to release the DMSA that did not react with the SPIONs a dialysis was made using 4 RC Dialysis Membrane Tubing 12 to 14 kDa MWCO (Spectrum™ Spectra/Por™). The dialysis is finished when the water pH reaches 7.

B.

Iron content dtermination using 1,10-phenantrolin colorimetrmethod

The produced SPIONs were diluted in Millipore water in a 1:100 ratio in an Eppendorf tube. Then, 40 µL of that dilution were transferred to another Eppendorf to which was added 20 µL of HCl 37% (v/v) (*Sigma-Aldrich*) and left for 1 hour for incubation, to dissolve all SPIONs and obtain ferrous and ferric chloride. Afterwards, solutions of hydroxylamine hydrochloride (100 mg/mL), 1,10-phenanthroline monohydrate (3 mg/mL) and ammonium acetate (500 mM) (all from Sigma-Aldrich) were prepared in 0.01 M HCl and then added to the Eppendorf, 100 µL, 500 µL and 1800 µL respectively. The absorbance of the samples was measured on the spectrophotometer (T90+ UV/VIS Spectrometer PG Instruments Ltd) at 510 nm using a HCl 0.01 M base line, resulting Abs (510 nm) = 3.5228 x ([Fe] mg/mL) + 0.0583, from the calibration curve. To obtain the nanoparticles concentration, the formula [Fe] = 0.7 x [NPs] was used [53].

C.
Cell culture

Table C: **Description of the Cellular assay:** type of assay, cell density that was seeded, type of plate used, volume of medium, and type of substrate, substrate concentration and its incubation time.

Assay	Cell density (cells/cm²)	Well plate	Medium volume (µL)	Substrate	Substrate concentration	Incubation time
Resazurin	30000	96 wells	100	SPIONs	0.03, 0.06, 0.125, 0.500, 1, 2 mg/mL	24 h
Resazurin	30000	96 wells	100	H_2O_2	20 mM, 5 mM, 50 µM	24 h
Live/Dead	50000	12 wells	500	SPIONs_ APTES	0.03, 0.06, 0.125, 0.500, 1, 2 mg/ mL	24 h
Prussian Blue internalization	90000	24 wells	500	SPIONs	0.03 mg/mL	1,3,6,16,24 h
Intracellular quantification	90000	24 wells	500	SPIONs	0.03 mg/mL	1,3,6,16,24 h
Resazurin Catalase	30000	96 wells	1000	SPIONs + H_2O_2	0.03 mg/mL SPIONs + 50 µM H_2O_2	SPIONs: 24 h H_2O_2: 90, 60 and 30 min

D.
Cytotoxicity protocols: Resazurin assay and Live/Dead assay

Resazurine assay

Following cell culture with the addition of the substrate, the medium was discarded, and the cells were washed 3-5 times with culture medium until the nanoparticles precipitate disappeared. Then, 100 µL of a mixture containing equal parts of fresh culture medium and resazurin (0.04 g/L) was added to each well. Negative control cells were treated similarly and were incubated with the respective medium at the same dilution as the one used for incubation with nanoparticles. Positive control cells were treated with 10% Dimethyl Sulfoxide (DMSO) (Merck) to provoke cellular death. The plates were incubated for three hours, and the absorbance was measured at 570 nm (resorufin peak) and 600 nm (resazurin peak) in the microplate reader (Biotek ELX 800UV). Cell viability can be expressed as a percentage of the control, given by [% cell viability = NP treated cells/control cells × 100] [37].

Live/Dead assay

After cell culture and SPIONs internalization, cells were incubated with a solution containing 0.2 µL/mL of calcein (green dye live cell indicator, Biotium) and 0.8 µL/mL ethidium homodimer (red dye dead cell indicator, Biotium) with serum free Dulbecco´s Modified Eagle´s Medium (DMEM) with 25 mM of 4-(2-hydroxyethyl)-1-piperazineethanesulfonic acid (HEPES), for 30 min. Then the cells were washed with cell culture medium with Fetal bovine serum (FBS) in order to stop the fluorophore action. The percentage of live and dead cells was obtained through image analysis, given by [% cells = cell count/untreated control cell count x 100]. At least 10 images of each condition were taken by epifluorescence microscopy using a Nikon Inverted microscope with 10x magnification.

E.

Cellular uptake studies

Prussian Blue internalization assay

After cell culture and SPIONs internalization, we proceeded to fixation in coverslips and permeabilization, the cells were treated with 400 µL of Perl's reagent (4% potassium hexacyanoferrate (II) trihydrate, $K_4[Fe(CN)_6] \cdot 3H_2O$ (w/v) (Merck) and 4% of HCl (v/v) for a period of 40 minutes. After this time, the wells were rinsed 4 times with PBS and counterstained with 500 µL of nuclear fast red solution (Nuclear fast red 0.1% in 5% aluminum sulfate) (Sigma-Aldrich). Lastly, the wells were again washed 4x with PBS and the coverslips were withdraw from the wells. Each coverslip was washed with PBS and water and mounted in slides over 10 µL Mowiol Mounting medium (Sigma-Aldrich). All images were acquired with Nikon Inverted Microscope with transmitted-light bright field using a 20x objective magnification. At least 10 images of each condition were taken.

Intracellular quantification

After 1 h, 3 h, 6 h, 16 h and 24 h period of incubation, with the SPIONs 0.03 mg/mL the cells were detached from each well and placed in eppendorf tubes containing 500 µL of McCoy medium and washed with PBS by centrifugation at 1200x*g* for 3 minutes (this procedure was repeat 2 times). The supernatant was discarded, and cell pellet obtained was rapidly lysed in 500 µL HCl 37% (v/v) (*Panreac*) and incubated for 1 hour. In addition to promoting the cell lysis the hydrochloric acid acts to promote the conversion of all the SPIONs and obtain ferrous and ferric chloride. Lastly, 40 µL of lysed solution were placed in a new eppendorf tube and used to start the 1,10-phenantroline colorimetric method described in appendix B following the same steps as discriminated in that section without any alteration. Absorbance of all samples was measured at 510 nm using a UV-Vis spectrophotometer (T90+ UV/VIS Spectrometer PG Instruments Ltd).